

# UC San Diego

## UC San Diego Previously Published Works

### Title

Hippocampal neuronal cells that accumulate  $\alpha$ -synuclein fragments are more vulnerable to A $\beta$  oligomer toxicity via mGluR5--implications for dementia with Lewy bodies.

### Permalink

<https://escholarship.org/uc/item/5j9621m9>

### Journal

Molecular neurodegeneration, 9(1)

### ISSN

1750-1326

### Authors

Overk, Cassia R  
Cartier, Anna  
Shaked, Gideon  
et al.

### Publication Date

2014-05-01

### DOI

10.1186/1750-1326-9-18

Peer reviewed

RESEARCH ARTICLE

Open Access

# Hippocampal neuronal cells that accumulate $\alpha$ -synuclein fragments are more vulnerable to A $\beta$ oligomer toxicity via mGluR5 – implications for dementia with Lewy bodies

Cassia R Overk<sup>1</sup>, Anna Cartier<sup>1</sup>, Gideon Shaked<sup>1</sup>, Edward Rockenstein<sup>1</sup>, Kiren Ubhi<sup>1</sup>, Brian Spencer<sup>1</sup>, Diana L Price<sup>2</sup>, Christina Patrick<sup>1</sup>, Paula Desplats<sup>1</sup> and Eliezer Masliah<sup>1,3\*</sup>

## Abstract

**Background:** In dementia with Lewy bodies (DLB) abnormal interactions between  $\alpha$ -synuclein ( $\alpha$ -syn) and beta amyloid (A $\beta$ ) result in selective degeneration of neurons in the neocortex, limbic system and striatum. However, factors rendering these neurons selectively vulnerable have not been fully investigated. The metabotropic glutamate receptor 5 (mGluR5) has been shown to be up regulated in DLB and might play a role as a mediator of the neurotoxic effects of A $\beta$  and  $\alpha$ -syn in vulnerable neuronal populations. In this context, the main objective of the present study was to investigate the role of mGluR5 as a mediator of the neurotoxic effects of  $\alpha$ -syn and A $\beta$  in the hippocampus.

**Results:** We generated double transgenic mice over-expressing amyloid precursor protein (APP) and  $\alpha$ -syn under the mThy1 cassette and investigated the relationship between  $\alpha$ -syn cleavage, A $\beta$ , mGluR5 and neurodegeneration in the hippocampus. We found that compared to the single tg mice, the  $\alpha$ -syn/APP tg mice displayed greater accumulation of  $\alpha$ -syn and mGluR5 in the CA3 region of the hippocampus compared to the CA1 and other regions. This was accompanied by loss of CA3 (but not CA1) neurons in the single and  $\alpha$ -syn/APP tg mice and greater loss of MAP 2 and synaptophysin in the CA3 in the  $\alpha$ -syn/APP tg. mGluR5 gene transfer using a lentiviral vector into the hippocampus CA1 region resulted in greater  $\alpha$ -syn accumulation and neurodegeneration in the single and  $\alpha$ -syn/APP tg mice. In contrast, silencing mGluR5 with a lenti-shRNA protected neurons in the CA3 region of tg mice. *In vitro*, greater toxicity was observed in primary hippocampal neuronal cultures treated with A $\beta$  oligomers and over-expressing  $\alpha$ -syn; this effect was attenuated by down-regulating mGluR5 with an shRNA lentiviral vector. In  $\alpha$ -syn-expressing neuronal cells lines, A $\beta$  oligomers promoted increased intracellular calcium levels, calpain activation and  $\alpha$ -syn cleavage resulting in caspase-3-dependent cell death. Treatment with pharmacological mGluR5 inhibitors such as 2-Methyl-6-(phenylethynyl)pyridine (MPEP) and 3-((2-Methyl-4-thiazolyl)ethynyl)pyridine (MTEP) attenuated the toxic effects of A $\beta$  in  $\alpha$ -syn-expressing neuronal cells.

**Conclusions:** Together, these results support the possibility that vulnerability of hippocampal neurons to  $\alpha$ -syn and A $\beta$  might be mediated via mGluR5. Moreover, therapeutic interventions targeting mGluR5 might have a role in DLB.

**Keywords:**  $\alpha$ -synuclein, Amyloid  $\beta$  oligomer, Dementia with Lewy body, Hippocampus, Human, mGluR5, Parkinsonism, Transgenic animal model

\* Correspondence: [emasliah@ucsd.edu](mailto:emasliah@ucsd.edu)

<sup>1</sup>Department of Neurosciences, University of California, San Diego, La Jolla, CA, USA

<sup>3</sup>Department of Pathology, University of California, San Diego, La Jolla, CA, USA

Full list of author information is available at the end of the article

## Background

Alzheimer's disease (AD) and Parkinson's disease (PD) are the leading causes of dementia and movement disorders in the aging population. It is estimated that over 5 million people live with these devastating neurological conditions in the US [1]. While in AD abnormal accumulation of misfolded amyloid- $\beta$  protein (A $\beta$ ) in the neocortex and limbic system is responsible for the neurodegenerative pathology [2,3], in PD accumulation and propagation of  $\alpha$ -synuclein ( $\alpha$ -syn) has been centrally implicated in this condition [4-6]. The pathogenesis of AD and PD overlap in a heterogeneous group of conditions denominated jointly as Lewy body disease (LBD) [7,8], which includes dementia with Lewy bodies (DLB), Parkinson's disease with dementia (PDD) and idiopathic PD (iPD). Direct and indirect interactions between  $\alpha$ -syn and A $\beta$  play a role in the pathogenesis of LBD [9-13]. Specifically, A $\beta$  promotes the oligomerization and toxic conversion of  $\alpha$ -syn [12,14]; A $\beta$  worsens the deficits associated with  $\alpha$ -syn accumulation [15,16]; A $\beta$  and  $\alpha$ -syn co-localize in membrane and caveolar fractions [13]; and A $\beta$  stabilizes  $\alpha$ -syn multimers that might form heteromultimers in the membrane [13].

In DLB, neuronal populations degenerate in the neocortex, CA3 region of the hippocampus, and mid-spiny neurons in the striatum [17,18]. Among the cell-autonomous factors that might render neurons vulnerable in DLB to the combined effects of A $\beta$  and  $\alpha$ -syn, it has been proposed that the expression profile of mGluRs might be a determinant for the degeneration of the hippocampal formation and neurons in DLB [19]. Considerable interest in mGluR5 [20] has developed in the last few years due to: **1**) its potential involvement in AD [21] and PD [22,23], **2**) the role of this receptor in learning and memory [24,25], **3**) mGluR5 is abundantly expressed in the neocortex, limbic system and caudoputamen [26]—brain regions selectively affected in AD and PD, and **4**) selective inhibitors of mGluR5, 2-methyl-6-(phenylethynyl)pyridine (MPEP) and 3-((2-Methyl-4-thiazolyl)ethynyl)pyridine (MTEP), are currently being considered as potential therapies for neurodegenerative disorders [23].

mGluR5 is more abundant in the hippocampal pyramidal neurons, the nucleus accumbens, and striatum of the basal ganglia and granular cells in the olfactory bulb (OB) [27,28], and is expressed at low levels in the cerebellum [26]. In AD and DLB the mGluR/phospholipase C (PLC) signaling pathways are impaired [29]. Moreover, A $\beta$  dysregulates the PKC-dependent functions of mGluRs in cortical neurons [30] and the levels of mGluR5 are abnormal in AD patients, and are up regulated in the Down's syndrome brains [31].

Remarkably, we have shown that in DLB and PD patients and  $\alpha$ -syn transgenic (tg) mice there is increased

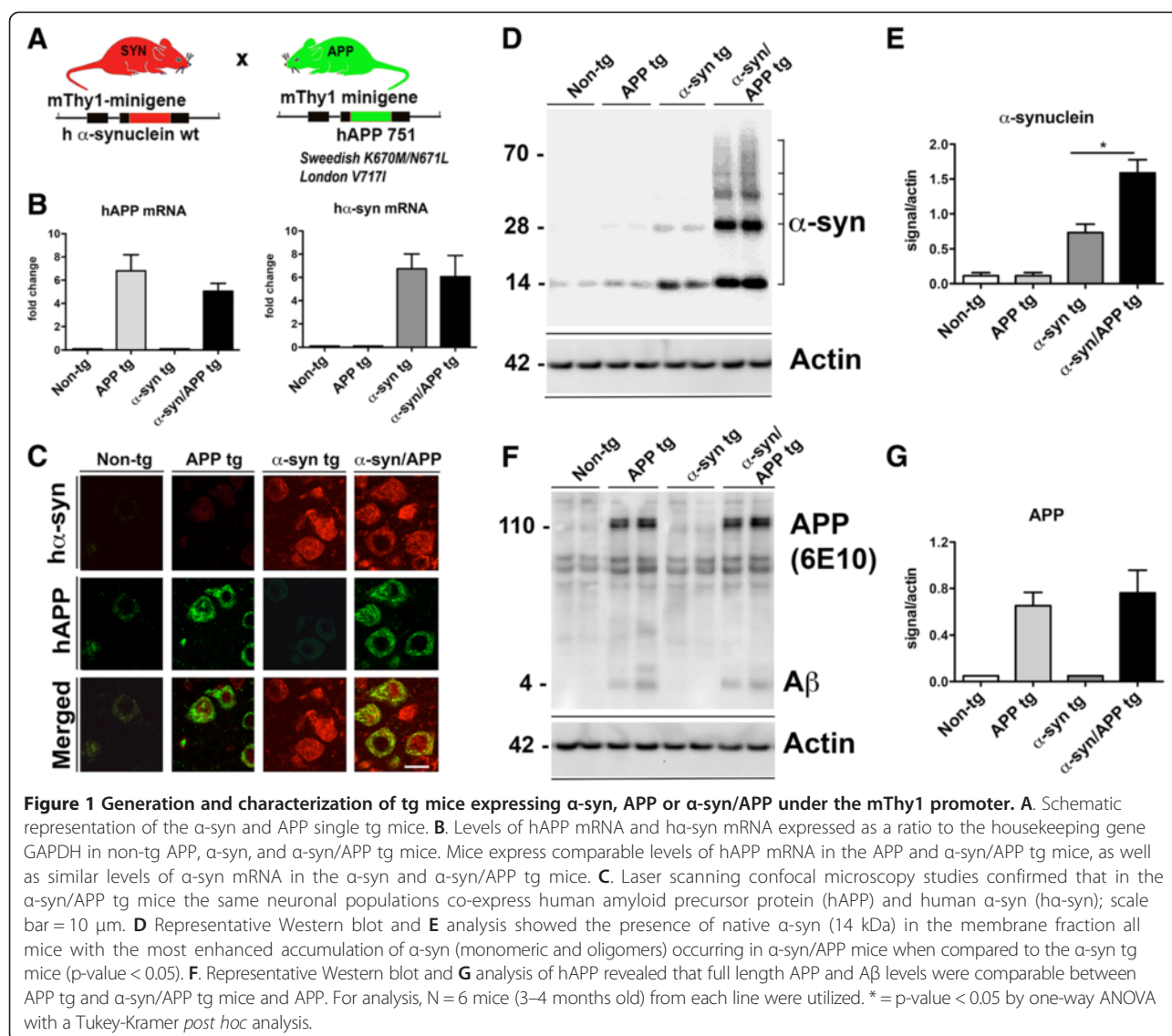
expression of mGluR5 in the hippocampus and striatum [19]. In the 1-methyl-4-phenyl-1,2,3,6-tetrahydropyridine (MPTP) model of dopaminergic damage, activation of mGluR5 contributes to the neurodegenerative process [32] and mGluR5 blockers, such as MPEP, protect neurons from MPTP and 6-OH dopamine (DOPA) challenge [33-35].

Taken together, these studies suggest that mGluR5 might play a role as a mediator of the neurotoxic effects of A $\beta$  and  $\alpha$ -syn in AD and PD. In this context, the main objective of the present study was to investigate the role of mGluR5 as a mediator of the neurotoxic effects of  $\alpha$ -syn and A $\beta$  in the hippocampus. We found that degeneration of the CA3 region of the hippocampus in  $\alpha$ -syn/APP double tg mice was associated with increased accumulation of  $\alpha$ -syn and increased expression of mGluR5. Down regulation of mGluR5 was protective while ectopic overexpression of mGluR5 in the CA1 resulted in neurodegeneration. In  $\alpha$ -syn expressing neuronal cell lines, A $\beta$  oligomers promoted increased intracellular calcium levels, calpain activation and  $\alpha$ -syn cleavage, resulting in caspase-3 dependent cell death. Together, these results support the possibility that vulnerability of hippocampal neurons to  $\alpha$ -syn and A $\beta$  might be mediated via mGluR5.

## Results

### Characterization and comparison of mRNA and protein expression in transgenic mouse lines expressing APP, $\alpha$ -syn and $\alpha$ -syn/APP

In order to understand the role of  $\alpha$ -syn and A $\beta$  in mediating neurodegeneration in the hippocampus via mGluR5, we generated  $\alpha$ -syn/APP double tg mice by crossing mThy1- $\alpha$ -syn (Line 61) and mThy-1 APP (Line 41) (Figure 1A). We chose to cross these two specific tg lines to ensure co-expression of APP and  $\alpha$ -syn in the same neuronal populations, at comparable levels, and because each individual line has shown robust pathology in vulnerable areas relevant to AD and PD [36,37]. Quantitative PCR (qPCR) analysis of mRNA isolated from brain tissue demonstrated the presence of comparable levels of hAPP mRNA in the APP and  $\alpha$ -syn/APP tg mice (Figure 1B). Analysis of the same brain tissues for  $\alpha$ -syn mRNA revealed comparable levels of h $\alpha$ -syn in both  $\alpha$ -syn single tg and the  $\alpha$ -syn/APP double tg mouse lines (Figure 1B). Double labeling and laser scanning confocal microscopy studies confirmed that in the  $\alpha$ -syn/APP tg mice the same neuronal populations co-express human amyloid precursor protein (hAPP) and human  $\alpha$ -syn (h $\alpha$ -syn) (Figure 1C). Consistent with the mRNA and immunohistochemical analysis, Western blot experiments also confirmed the presence of the native  $\alpha$ -syn band at approximately 14 kDa in the non-tg and tg mice lines. In line with previous studies [9,12], the  $\alpha$ -syn/APP



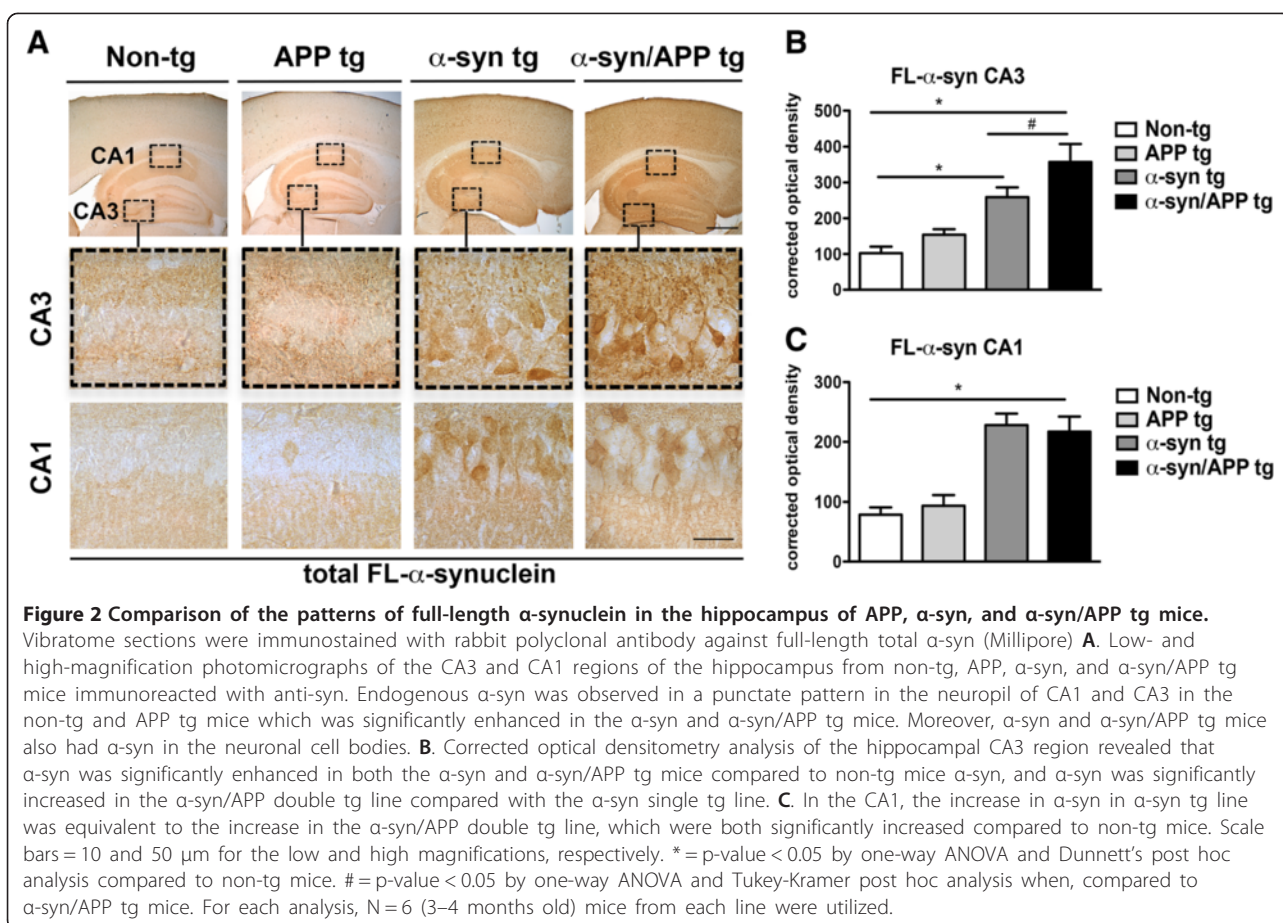
tg mice displayed greater accumulation of  $\alpha$ -syn (monomeric and oligomers) when compared to the  $\alpha$ -syn tg mice ( $p$ -value < 0.05; Figure 1D and E). Western blot evaluation of APP revealed that full length (FL-) APP and  $A\beta$  levels were comparable between APP tg and  $\alpha$ -syn/APP double tg mice (Figure 1F and G).

#### Full-length $\alpha$ -syn and mGluR5 are increased in the CA3 pyramidal layer of the hippocampus in $\alpha$ -syn/APP mice compared to $\alpha$ -syn tg mice

To investigate the effects of the co-expression of  $\alpha$ -syn and APP on mGluR5 levels in the hippocampus, immunocytochemical and image analysis was performed. We focused on the hippocampus because in previous studies we showed that the levels of mGluR5 were up regulated in the CA3 in a different single tg  $\alpha$ -syn mouse

line [19]. As expected, utilizing an antibody against total full-length  $\alpha$ -syn that revealed the endogenous punctate pattern in the neuropil of the CA1 and CA3 regions in the non-tg and APP single tg mice (Figure 2A). In contrast, in the  $\alpha$ -syn tg and  $\alpha$ -syn/APP double tg mice  $\alpha$ -syn was present in the neuronal cell bodies and had a significantly enhanced punctate pattern in the neuropil (Figure 2). In the CA3 there was a statistically significant increase in  $\alpha$ -syn in the  $\alpha$ -syn/APP double tg line compared with the  $\alpha$ -syn single tg line ( $p$ -value < 0.05; Figure 2A and B); while in the CA1, the increase in  $\alpha$ -syn in  $\alpha$ -syn tg line was equivalent to the increase in the  $\alpha$ -syn/APP double tg line, which were both significantly increased compared to non-tg mice ( $p$ -value < 0.05; Figure 2A and C).

Immunocytochemical analysis of mGluR5 revealed endogenous punctate pattern in the neuropil of non-tg mice



in both the CA1 and CA3. As expected, in APP and α-syn single tg mice, mGluR5 was significantly increased in the cell bodies, as well as in the punctate pattern of the neuropil in the CA3 compared to non-tg mice (p-value < 0.05; Figure 3A and B). In α-syn/APP double tg mice, mGluR5 levels were statistically enhanced (p-value < 0.05) compared to α-syn single tg mice in the CA3, with mGluR5 increased in both the neuronal cell bodies, as well as in the neuropil (Figure 3A and B). While mGluR5 levels were increased in the CA3 across all tg lines, there was no increase in the CA1 compared to non-tg mice (Figure 3A and C), suggesting that the CA3 is selectively vulnerable to alterations in mGluR5 levels. Since there was an increased expression of mGluR5 in the CA3 pyramidal cell layer in α-syn/APP double tg mice, which paralleled the increase in FL-α-syn expression in the CA3 pyramidal cell layer of α-syn/APP mice compared to α-syn mice, sections were double-labeled for α-syn and mGluR5. Confocal microscopy of the CA3 pyramidal cell layer of the hippocampus confirmed that mGluR5 was increased in the presence of, and co-localized with, α-syn in both the α-syn tg and α-syn/APP double tg mouse lines compared to APP tg and non-tg mice (Figure 3D).

#### Hippocampal CA3 but not CA1 pyramidal cells selectively vulnerable in APP, α-syn, and α-syn/APP tg mice

Based on the observation that mGluR5 and FL-α-syn are increased in the CA3 but not CA1, stereological analysis was performed to determine if the CA3 was selectively vulnerable to neurodegeneration in the APP, α-syn and α-syn/APP tg mouse lines (Figure 4). The number of NeuN-positive cells in the CA3 was significantly decreased by approximately 50% across all tg mouse lines (p-value < 0.05; Figure 4B) but remained unaffected in the CA1 pyramidal cell layer (Figure 4C). To further investigate the selective neurodegeneration in the hippocampal CA3 pyramidal layer, immunocytochemical analysis was performed with other markers including MAP 2 (dendritic marker), synaptophysin (pre-synaptic terminal marker), GFAP (astroglial cells), and Iba-1 (microglial cells). In the CA3 region of the non-tg mice, MAP 2-immunoreactivity (–ir) was found in the neuronal cell bodies and dendrites using confocal microscopy. In contrast, APP, α-syn and α-syn/APP tg mice displayed a reduction on MAP 2 immunolabeling in the CA3 region (p-value < 0.05; Figure 5A and B). The most dramatic loss in MAP 2-ir was in the α-syn/APP double tg mice,



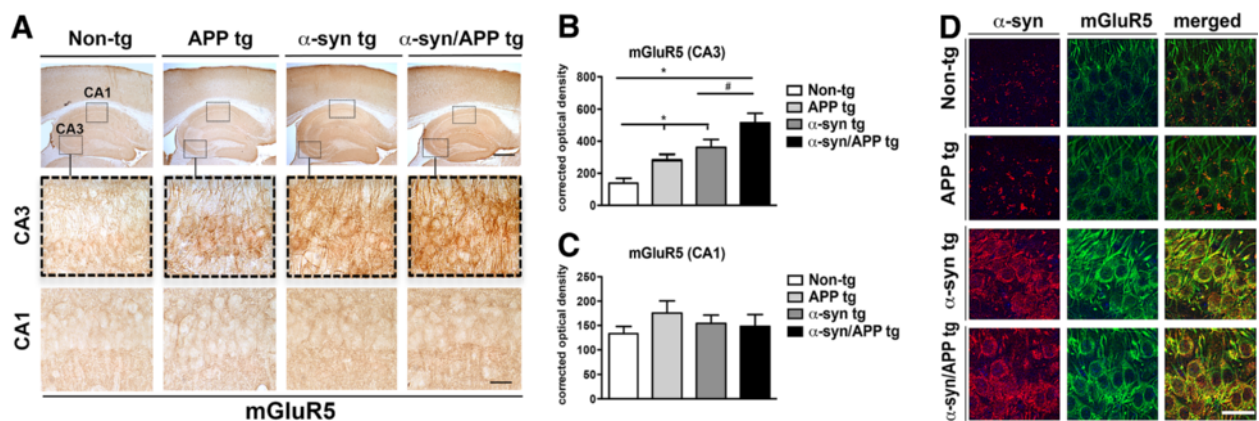


**Figure 3** Immunocytochemical analysis of mGluR5 in the hippocampus of APP,  $\alpha$ -syn, and  $\alpha$ -syn/APP tg mice. Vibratome sections were immunostained with an antibody against mGluR5. **A**, Low- and high-magnification photomicrographs of the CA3 and CA1 regions of the hippocampus from non-tg, APP,  $\alpha$ -syn, and  $\alpha$ -syn/APP tg mice immunoreacted with anti-mGluR5. Endogenous mGluR5 was observed in a punctate pattern in the neuropil of CA1 and CA3 in the non-tg mice. In the CA3, but not the CA1 the APP,  $\alpha$ -syn, and  $\alpha$ -syn/APP tg mice had mGluR5 in the neuronal cell bodies, and the punctate staining in the neuropil was significantly enhanced. **B**, Corrected optical densitometry analysis of the hippocampal CA3 region revealed that mGluR5 was significantly enhanced across all tg mice compared to non-tg mice  $\alpha$ -syn, and mGluR5 was significantly increased in the  $\alpha$ -syn/APP double tg line compared with the  $\alpha$ -syn single tg line. **C**, In the CA1, there was no significant difference in the amount of mGluR5 in any of the tg line compared to the non-tg line. **D**, Confocal imaging of CA3 hippocampus double-labeled with  $\alpha$ -syn and mGluR5 confirmed the presence and increase in mGluR5 with  $\alpha$ -syn in both the  $\alpha$ -syn and  $\alpha$ -syn/APP tg mice. Scale bars = 10 and 50  $\mu$ m for the low and high magnifications, respectively. \* = p-value < 0.05 by one-way ANOVA and Dunnett's post hoc analysis compared to non-tg mice. # = p-value < 0.05 by one-way ANOVA and Tukey-Kramer post hoc analysis when, compared to  $\alpha$ -syn/APP tg mice. For each analysis, N = 6 (3–4 months old) mice from each line were utilized.

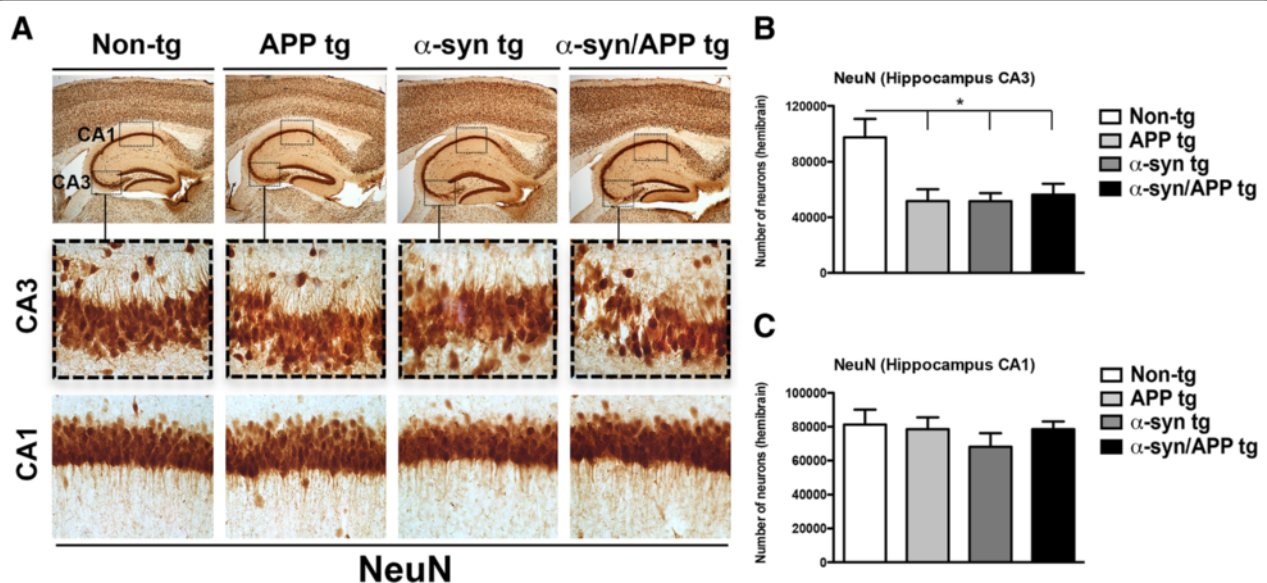
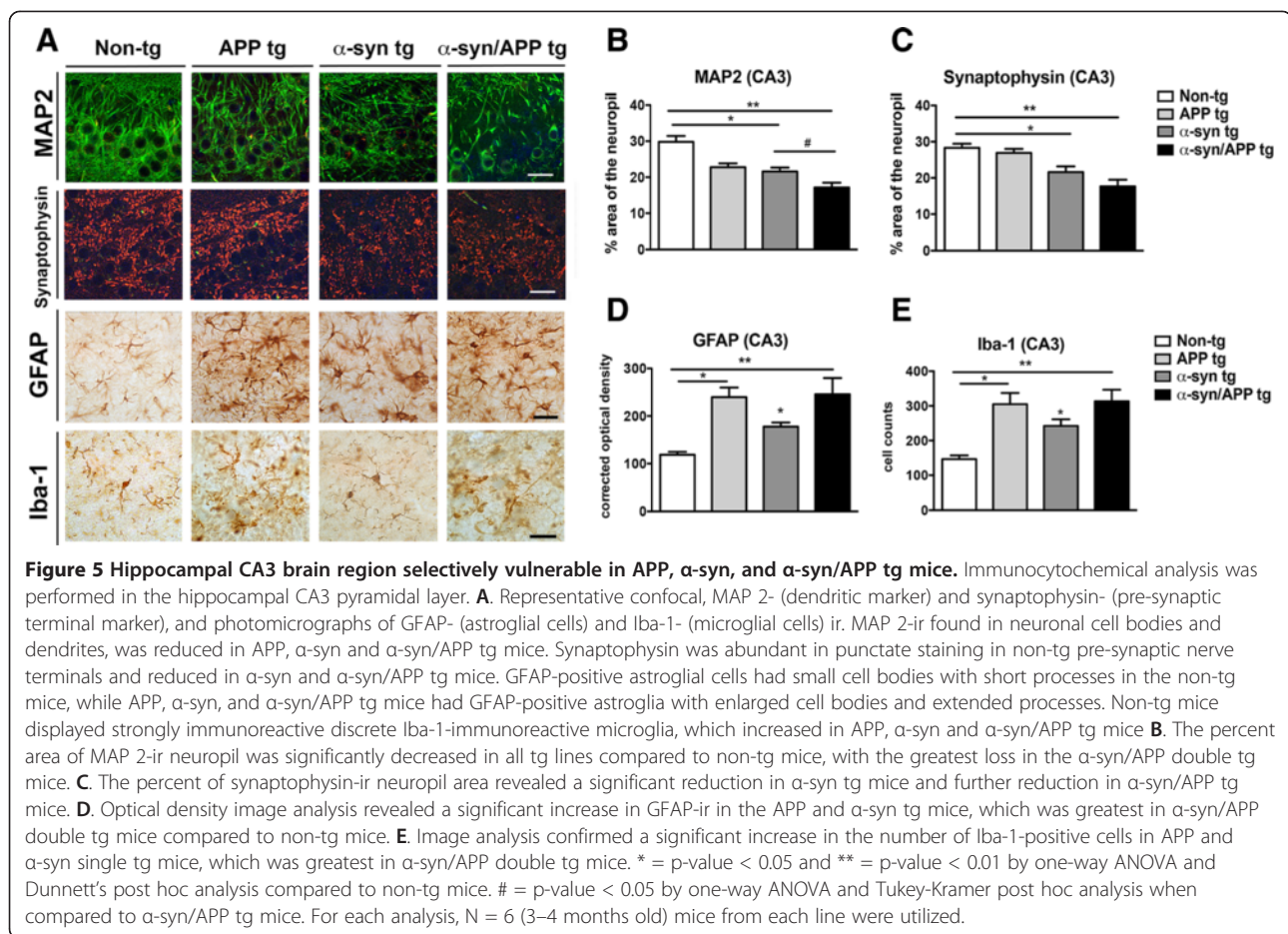


**Figure 4** Decreased number of hippocampal CA3 but not CA1 pyramidal cells in APP,  $\alpha$ -syn, and  $\alpha$ -syn/APP tg mice. **A**, Representative low- and high-magnification photomicrographs of the hippocampal CA3 and CA1 regions of sections immunoreacted with NeuN. **B**, Stereological assessment of every 12<sup>th</sup> section revealed a significant decrease in the number of neurons in the CA3. **C**, However, the number of neurons in the CA1 region was unaffected across all tg mouse line. Statistical analysis was conducted using one-way ANOVA post hoc Dunnett's compared to non-tg mice; \* p-value < 0.05. For analysis N = 3 (3–4 mos old) from each line were utilized.



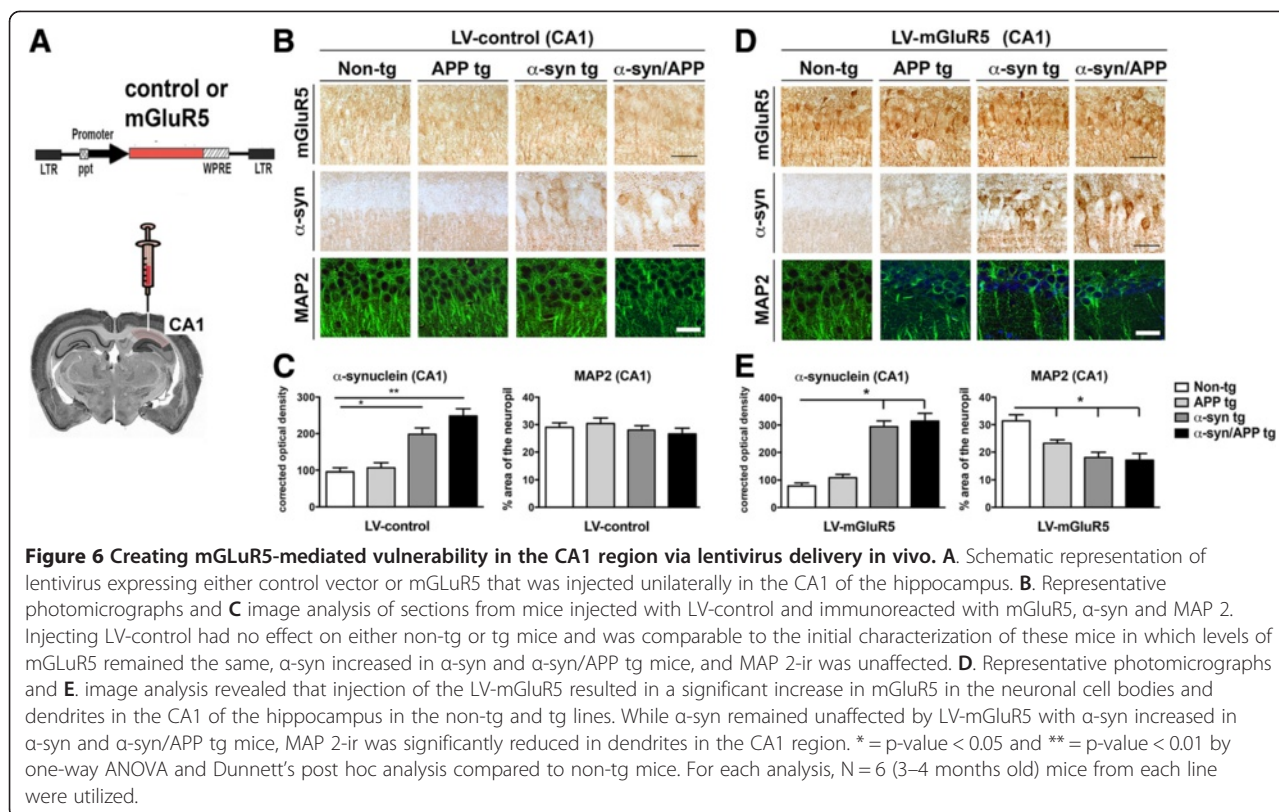
which showed a significant decrease in MAP 2-ir in the neuropil, both compared to non-tg mice (p-value < 0.01), as well as compared to α-syn single tg mice (p-value < 0.05; Figure 5A and B). Confocal microscopy and image analysis of synaptophysin in CA3 revealed abundant punctate staining in the pre-synaptic nerve terminals of non-tg mice (Figure 5A). While there was not much difference between in synaptophysin levels in non-tg and APP mice, the area of the neuropil that was synaptophysin-positive was significantly reduced in α-syn tg mice (p-value < 0.05) and even further reduced in the α-syn/APP tg mouse line (p-value < 0.01) in the CA3 of the hippocampus (Figure 5A and C).

While the non-tg mice had GFAP-positive astroglial cells within small cell bodies and short processes, APP, α-syn, and α-syn/APP tg mice had GFAP-positive astroglia with enlarged cell bodies and extended processes (Figure 5A). Optical density image analysis revealed a significant increase in GFAP-ir in the APP (p-value < 0.05) and α-syn (p-value < 0.05), with the greatest increase in α-syn/APP double tg mice (p-value < 0.01) compared to non-tg mice in the CA3 region (Figure 5A and D). Non-tg mice displayed the presence of discrete Iba-1-

immunoreactive microglia (Figure 5A). In the tg lines, morphological analysis revealed that APP, α-syn and α-syn/APP mice contained Iba-1-positive processes that were strongly immunoreactive with increased staining of microglia processes. Image analysis confirmed a significant increase in the number of Iba-1-positive cells in APP (p-value < 0.05) and α-syn (p-value < 0.05) single tg mice, which was most increased in α-syn/APP double tg mice (p-value < 0.05) in the CA3 region (Figure 5E).

#### Lentivirus mediated delivery of mGluR5 *in vivo* in the CA1 region is associated with increased vulnerability in a previously unaffected region

To investigate if increasing the levels of mGluR5 results in enhanced vulnerability of un-affected regions in the hippocampus, lentiviruses expressing either a control vector or mGluR5 was injected into the CA1 region of non-tg and tg mice (Figure 6A). As expected, following the injection of the lentivirus (LV) control, the levels and patterns of mGluR5 immunostaining in the CA1 were comparable among the non-tg and tg lines. Levels of α-syn were higher in the α-syn and α-syn/APP and comparable in the non-tg and APP tg mice (Figure 6B and C).



Likewise the percent area covered by MAP 2 dendrites in the CA1 was similar among non-tg and tg lines (Figure 6B and C). In contrast, injection of the LV-mGluR5 resulted in a significant increase in mGluR5 in the neuronal cell bodies and dendrites in the CA1 of the hippocampus in the non-tg and tg lines (Figure 6D). There was a significant accumulation of  $\alpha$ -syn in the CA1 region in the  $\alpha$ -syn and  $\alpha$ -syn/APP tg mice compared to non-tg and APP tg mice (Figure 6D and E). Moreover the accumulation of  $\alpha$ -syn in the tg lines was greater in mice injected with LV-mGluR5 when compared to mice injected with the LV-control in the CA1 region. Confocal analysis of MAP 2 in the CA1 region showed that compared to the non-tg mice, APP and  $\alpha$ -syn and  $\alpha$ -syn/APP tg mice that were injected with LV-mGluR5 resulted in significant reduction of dendrites in the CA1 region (Figure 6D and E). Taken together, these results supports the possibility that increased expression of mGluR5 in the CA3 plays a role in the vulnerability of this region in tg mice and that ectopic over-expression of mGluR5 in the CA1 results in neurodegeneration.

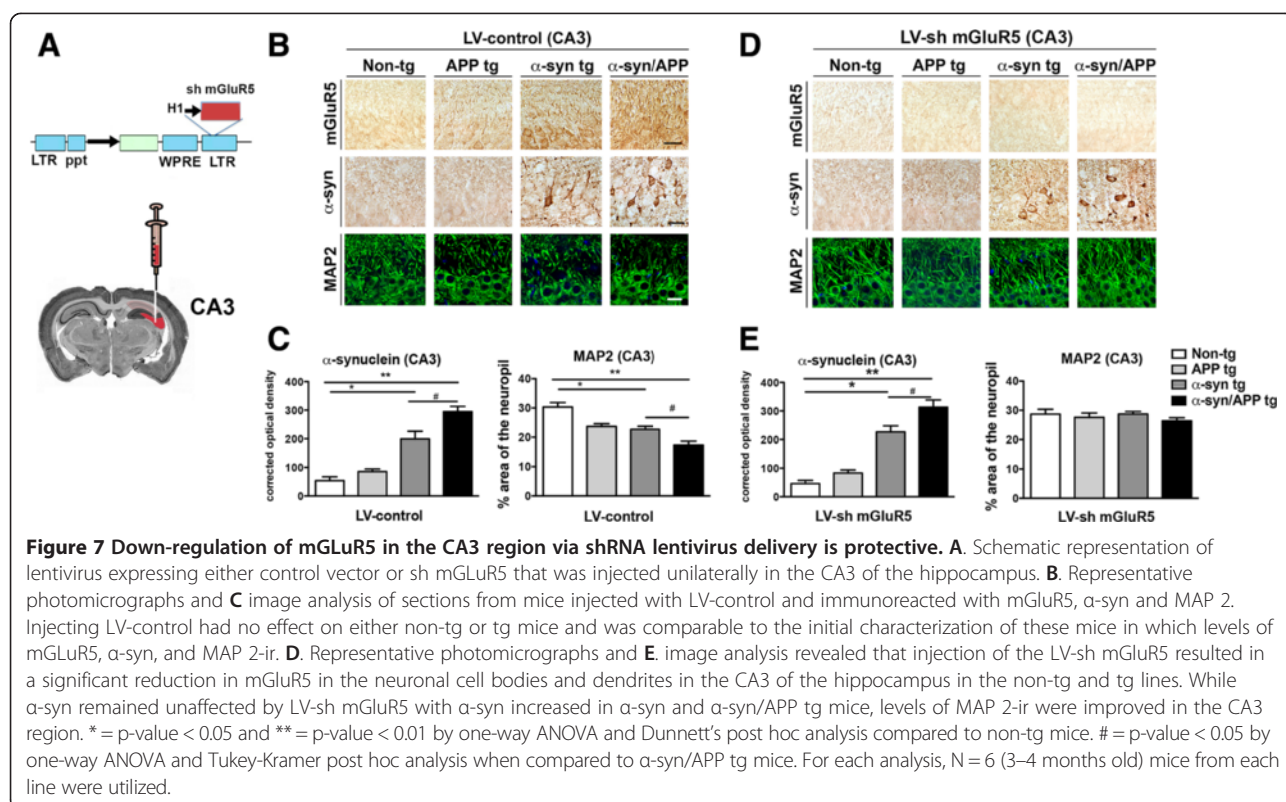
#### Down-regulation of mGluR5 with a lentivirus sh-RNA protects hippocampal neuronal cells from the neurotoxic effects of A $\beta$ and $\alpha$ -syn

Next we wanted to ascertain if down-regulating mGluR5 in the hippocampus would be protective in models of A $\beta$

and  $\alpha$ -syn toxicity. To investigate if reducing the levels of mGluR5 results in decreased toxicity in the hippocampus, lentiviruses expressing either a control vector or sh-mGluR5 was injected into the CA3 region of non-tg and tg mice (Figure 7A). In the LV-control group, the levels of mGluR5 were higher in the CA3 in the  $\alpha$ -syn and  $\alpha$ -syn/APP and comparable in the non-tg and APP tg mice (Figure 7B and C). The percent area covered by MAP 2 dendrites in the CA3 was significantly reduced in the APP,  $\alpha$ -syn and  $\alpha$ -syn/APP compared to non-tg and tg lines (Figure 7B and C). In contrast, injection of the LV-sh mGluR5 resulted in a significant decrease in mGluR5 in the neuronal cell bodies and dendrites in the CA3 of the hippocampus in the non-tg and tg lines (Figure 7D). There was a significant accumulation of  $\alpha$ -syn in the CA3 region in the  $\alpha$ -syn and  $\alpha$ -syn/APP tg mice compared to non-tg and APP tg mice (Figure 7D and E). Confocal analysis of MAP 2 in the CA3 region showed that % area of the neuropil was comparable between the non-tg mice and the APP and  $\alpha$ -syn and  $\alpha$ -syn/APP tg (Figure 7D and E). Taken together, these results support the notion that reduced expression of mGluR5 in the CA3 is protective.

To confirm the effects in an independent system *in vitro*, primary hippocampal neuronal cells were infected with an LV-sh-mGluR5 or LV-sh-Luc (control targeting luciferase) in combination with A $\beta$  and  $\alpha$ -syn. First we evaluated the expression of mGluR5; as expected, cells injected with





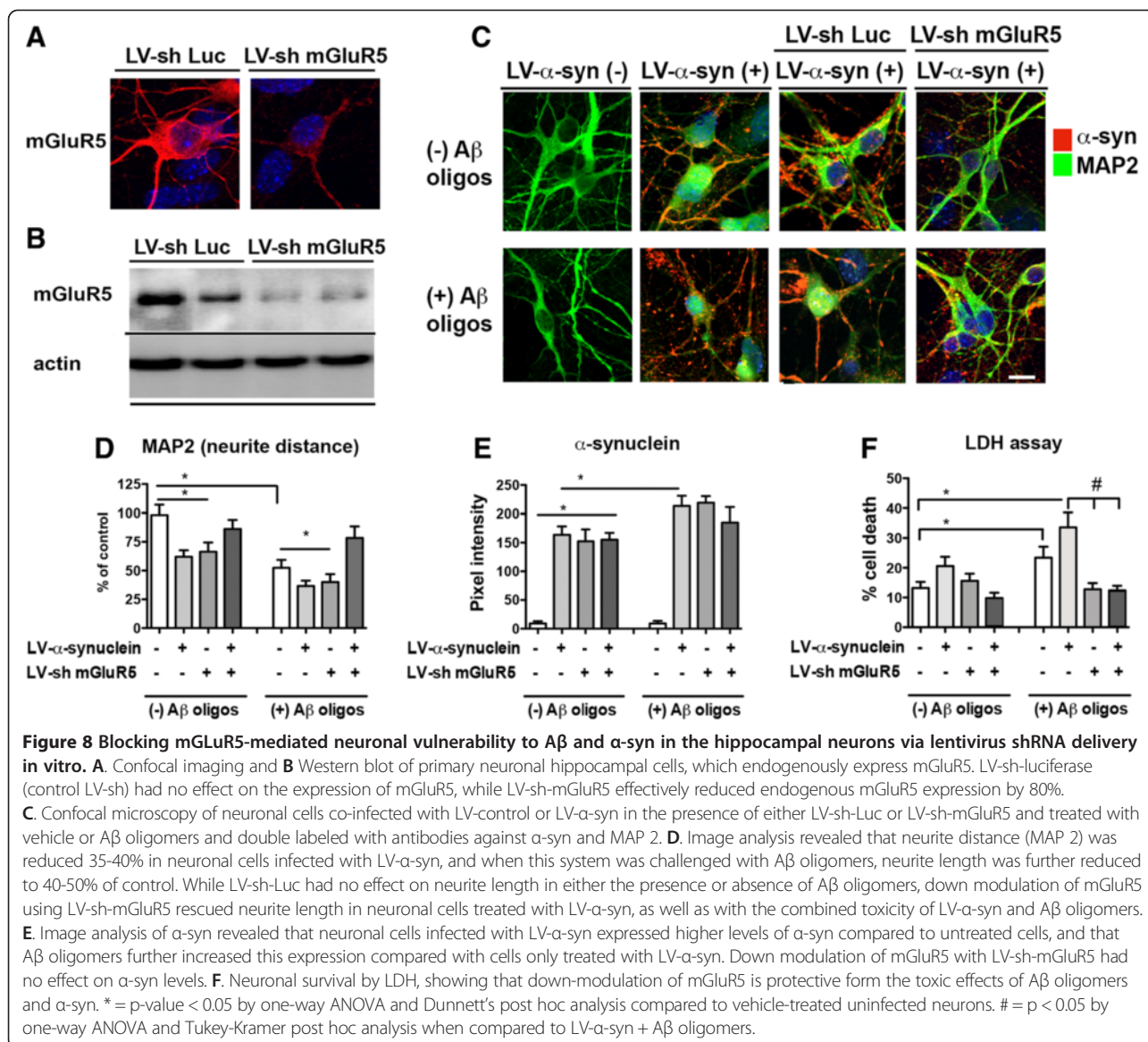
LV-sh-Luc control expressed high levels of mGluR5 by immunocytochemistry (Figure 8A) and Western blot (Figure 8B). In contrast, cells infected with the LV-sh-mGluR5 displayed a significant 80% reduction in mGluR5 expression (Figure 8B). Next neuronal cells were co-infected with a LV-control or LV- $\alpha$ -syn and treated with vehicle or A $\beta$  oligomers and analyzed by confocal microscopy for neuritic processes and  $\alpha$ -syn levels (Figure 8C). Compared to the control, neuronal cells infected with LV- $\alpha$ -syn displayed 35-40% reduction in neurite length (Figure 8C and D), likewise neuronal cells infected with LV-control and challenged with A $\beta$  oligomers alone resulted in 40-50% loss in neurite length that was worsened in cells infected with LV- $\alpha$ -syn (Figure 8C and D). Compared to control experiments using LV-sh-Luc, down modulation of mGluR5 with LV-sh-mGluR5 rescued the neuritic phenotype in both neuronal cells infected with LV- $\alpha$ -syn alone, treated with A $\beta$  oligomers alone or in combination (Figure 8C and D). As expected neuronal cells infected with LV- $\alpha$ -syn expressed higher levels of  $\alpha$ -syn (Figure 7C and E). Compared to vehicle treated cells, levels of  $\alpha$ -syn were higher in infected cells treated with A $\beta$  oligomers (Figure 8C and E). Down modulation of mGluR5 with LV-sh-mGluR5 had no effects on levels  $\alpha$ -syn (Figure 8E). By LDH assay, compared to the control, neuronal cells infected with LV-control and challenged with A $\beta$  oligomers alone resulted in greater neuronal cell death that was worsened in cells infected with LV- $\alpha$ -syn

(Figure 8F). Compared to control experiments using LV-sh-Luc, down modulation of mGluR5 with LV-sh-mGluR5 protected neurons from the toxic effects of A $\beta$  oligomers and - $\alpha$ -syn (Figure 8F).

#### A $\beta$ and $\alpha$ -syn promotes cell death and abnormal calcium flux via mGluR5 in a neuronal cell line

Since previous have shown that mGluR5 might be involved in mediating the toxic effects of A $\beta$  [30,38-42], and mGluR5 deficient mice or mice treated with mGluR5 inhibitors are protected from MPTP-induced toxicity in models of parkinsonism [25,34,43], we tested the role of mGluR5 in mediating toxicity in our system. For this purpose, the co-pathogenic mechanisms of A $\beta$  and  $\alpha$ -syn toxicity were investigated in the B103 rat neuroblastoma cells that were infected with LV- $\alpha$ -syn and treated with A $\beta$  oligomers (10  $\mu$ M) for 24 h. Levels of mGluR5 were analyzed, both by immunocytochemistry (Figure 9A and B) and WB (Figure 9C). The LV-control infected cells expressed low levels of mGluR5; in contrast, neuronal cells infected with LV- $\alpha$ -syn and challenged with control media or A $\beta$  oligomers displayed an increase in mGluR5 levels over control (Figure 9C).

Since activation of mGluR5 results in increased intracellular calcium [20] and both  $\alpha$ -syn [44] and A $\beta$  [45,46] raise this ion, intracellular calcium was measured as previously described using fluorescence-based assay, FLIPR (Molecular Devices). In the LV-control infected cells,

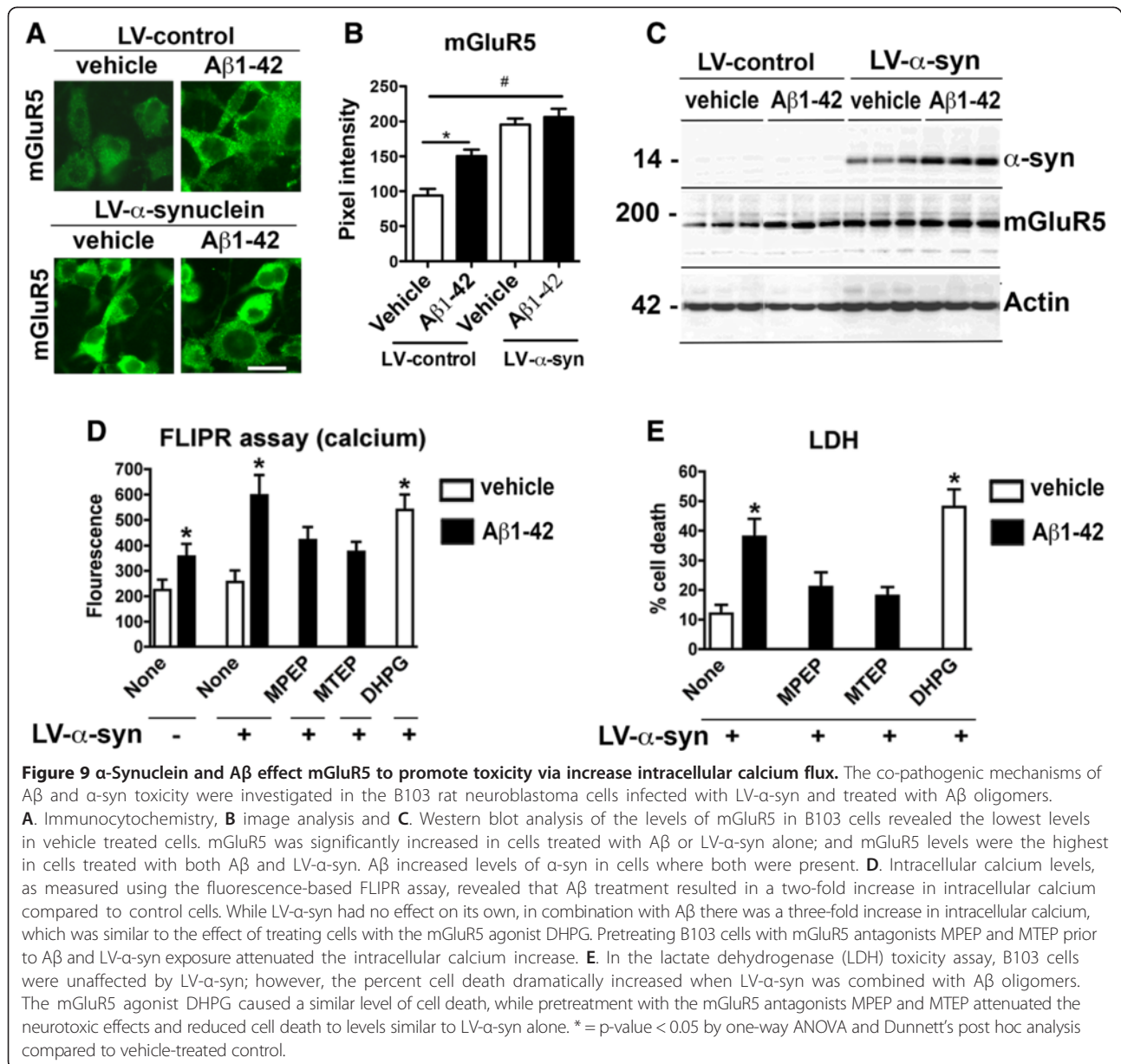


Aβ-treated cells displayed an approximate two-fold increase in intracellular calcium compared to control cells (Figure 9D). Treatment of LV-α-syn cells with the mGluR5 agonist- DHPG (1 μM, 24 h) showed similar results to the Aβ-treated group (Figure 9D). In the LV-α-syn infected cells, Aβ challenge resulted in approximate three-fold increase in intracellular calcium compared to control cells (Figure 9D). The combined effects of α-syn and Aβ on intracellular calcium levels were attenuated upon pre-treatment with the mGluR5 antagonists – MPEP (200 μM) and MTEP (20 μM) (Figure 9D). Using the lactate dehydrogenase (LDH) toxicity assay we found that while LV- α-syn infected cells displayed low toxicity, Aβ enhanced LV-α-syn toxicity to approximately three-times basal levels ( $p < 0.001$ ) comparable to the toxicity levels of the mGluR5 agonist -DHPG (Figure 9E). The combined

neurotoxic effects of LV-α-syn and Aβ were attenuated upon pre-treatment with the mGluR5 antagonists, MPEP and MTEP (Figure 9E). Together, these results support the possibility that α-syn and Aβ promote toxicity via increase intracellular calcium flux than in turn could activate proteases.

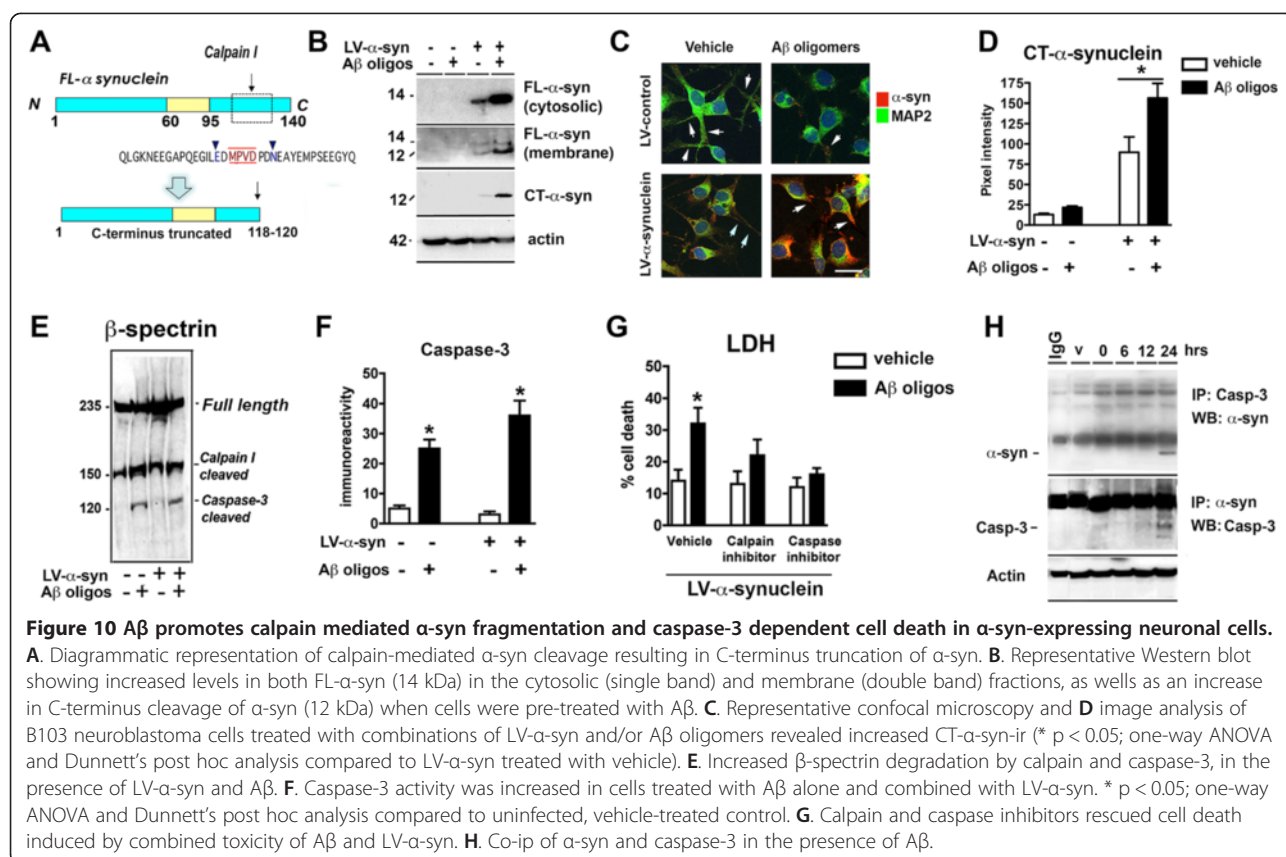
#### Aβ promotes calpain mediated α-syn fragmentation and caspase-3 dependent cell death in α-syn-expressing neuronal cells

Since previous studies suggest that intracellular calcium results in calpain-I activation and C-terminus cleavage of α-syn (Figure 10A), LV-α-syn infected B103 neuronal cells were treated with Aβ and analyzed by WB. Remarkably, in cells treated with Aβ (10 μM, 24 h), the levels of FL-α-syn in the cytosolic fraction (soluble) were



significantly increased (Figure 10B), while in the membrane fraction (insoluble) two immunoreactive bands were observed. An antibody specific for the C-terminal (CT) fragment of  $\alpha$ -syn [47] confirmed that the shorter fragment generated was a CT- $\alpha$ -syn (Figure 10B). By confocal microscopy, LV- $\alpha$ -syn infected B103 cells treated with A $\beta$  displayed increased CT- $\alpha$ -syn-ir (Figure 10C and D; p-value < 0.05). This suggests that proteolytic enzymes in the presence of A $\beta$  might cleaved  $\alpha$ -syn. Previous studies suggest that calpain-I (Figure 10A) might be involved in this process [48-51]. Consistent with this possibility, analysis of  $\beta$ -spectrin degradation by immunoblot showed that in LV- $\alpha$ -syn infected B103 cells treated with A $\beta$  had an increased generation of  $\beta$ -spectrin fragments

at 145/150 kDa and at 120 kDa (Figure 10E). FL  $\beta$ -spectrin is a 240 kDa protein, while a 145/150 kDa doublet is indicative of calpain cleavage, and the 120 kDa fragment is indicative of caspase-3 cleavage. The calpain-I mediated generation of CT  $\alpha$ -syn in A $\beta$ -treated cells was associated with activation of caspase-3 as revealed by immunocytochemical analysis (Figure 9F) and increased cell death by LDH (Figure 10G). Consistent with these findings, pre-treatment with calpain-I (calpeptin IV) or caspase-3 (z-DEVD-FMK) inhibitors significantly reduced cell death in LV- $\alpha$ -syn infected neuronal cells treated with A $\beta$  (Figure 10G). Moreover, after 24 h incubation, co-IP analysis showed that  $\alpha$ -syn interacts with caspase-3 (Figure 10H).



### Accumulation of CT α-syn and caspase-3 activation in α-syn/APP tg mice

To verify the effects on α-syn truncation in an *in vivo* model, Aβ and caspase-3 activation was determined using immunocytochemical and western blot analysis was performed. By confocal microscopy, APP and α-syn tg mice displayed a moderate increase in activated caspase-3-ir in the CA3 region of the hippocampus while the bigenic α-syn/APP mice showed an even greater increase compared to non-tg controls, (Figure 11A and B). Likewise, immunocytochemical analysis with an antibody against CT-α-syn showed a 0.5 to 1 fold increase in the single tg mice, while in the α-syn/APP tg mice displayed a 2.5 fold increase in the accumulation of CT-α-syn in the CA3 of the hippocampus (Figure 11C and D). By Western blot analysis using an antibody against CT-α-syn, detected a 12 kDa fragment at low levels in the single tg mice, while higher levels were detected in the α-syn/APP tg mice (Figure 11E and F). Moreover and consistent with the immunocytochemical analysis, levels of mGluR5 were higher in the α-syn and in the α-syn/APP tg mice compared to non-tg control mice (Figure 11E and F).

Taken together these results are in agreement with the *in vitro* experiments and suggest that vulnerability of hippocampal neurons to α-syn and Aβ might be mediated via

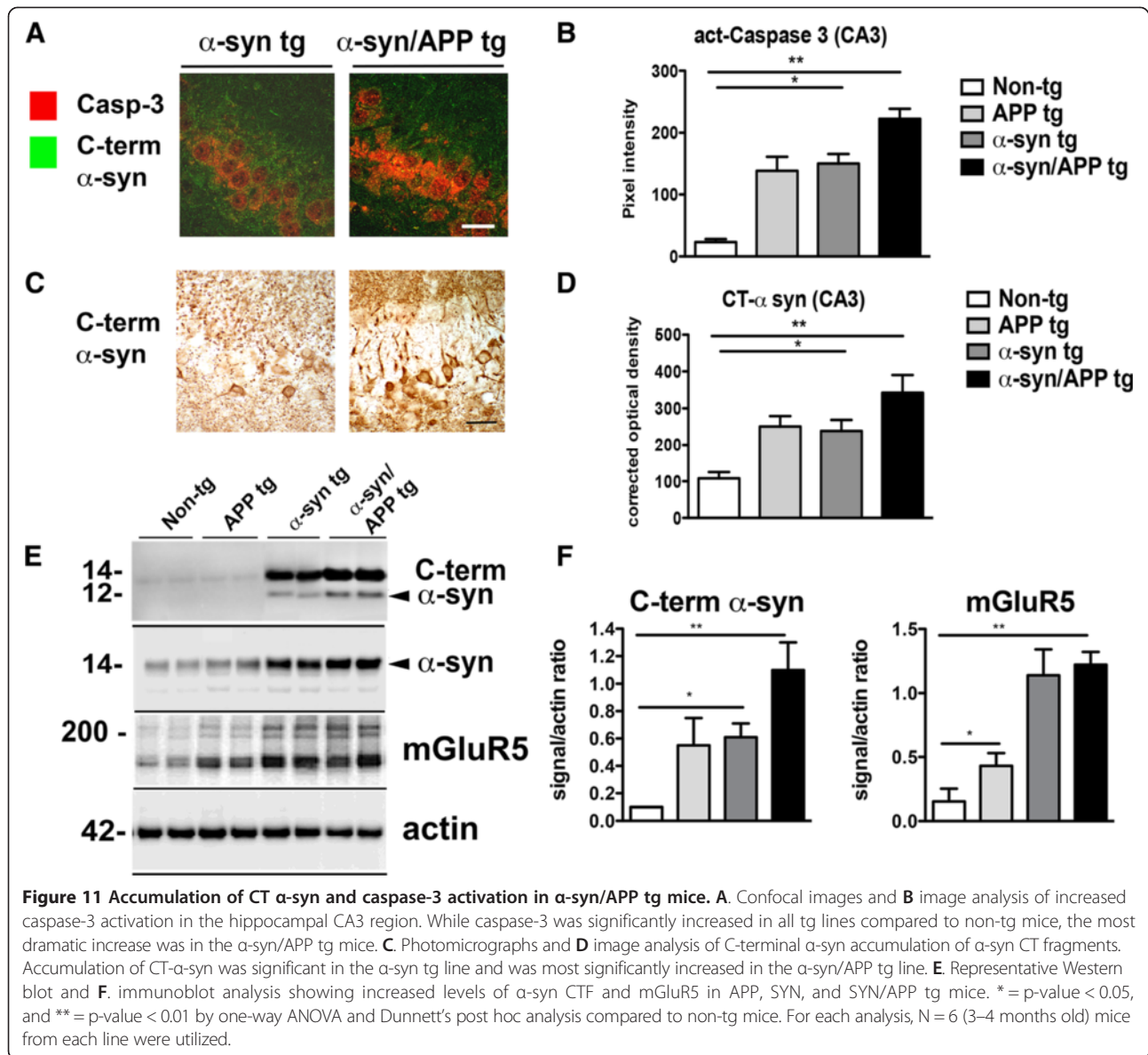
mGluR5 via calpain and caspase-3 activation resulting in CT-truncation of α-syn.

### Discussion

The present study showed that in single tg as well as in α-syn/APP tg mice the vulnerability of the CA3 region of the hippocampus to the combined effects of α-syn and Aβ are associated with increased mGluR5 and CT-α-syn accumulation. Moreover, while mGluR5 gene transfer into the CA1 region (that otherwise was preserved) resulted in neurodegeneration, silencing mGluR5 in the CA3 was protective in the single and α-syn/APP tg mice. In agreement with the *in vivo* studies, Aβ toxicity was enhanced in α-syn expressing neuronal cell cultures and the effect was attenuated by down-regulating mGluR5 with an shRNA lentiviral vector or pharmacologically with MPEP/MTEP. In α-syn expressing neuronal cells, Aβ oligomers promoted increased intracellular calcium levels, calpain-I activation and α-syn cleavage resulting in caspase-3 dependent cell death.

These findings are consistent with our previous study showing that mGluR5 is elevated in the hippocampus of DLB patients, as well as in α-syn tg mice [19]. While in the previous study we analyzed PDGF-α-syn (line D) mice [19], for this new study we investigated the mThy1-α-syn (line 61), as well as crosses with the mThy1-APP mutant





tg mouse model of DLB. This bigenic mThy1- $\alpha$ -syn/APP mutant tg line is new and has not been reported before. These lines were selected to ensure expression of  $\alpha$ -syn and APP in the same neuronal populations and because the high levels of expression in the hippocampus and the extent of the  $\alpha$ -syn and A $\beta$  pathology [36,37]. Thus while for the previous study we focused on the effects of  $\alpha$ -syn alone, for this study the emphasis was in investigating the combined effects of  $\alpha$ -syn and A $\beta$  and the downstream consequences on vulnerability and degeneration of hippocampal neurons. In the single and  $\alpha$ -syn/APP tg mice neurodegeneration was only observed in CA3 but not in CA1. In contrast, injection of LV-mGluR5 resulted in degeneration of the CA1 region, while down-regulating mGluR5 in tg mice and in neuronal cultures was

protective from the toxic effects of  $\alpha$ -syn and A $\beta$ . The mechanisms are not completely clear; however, one possibility is that  $\alpha$ -syn aggregates might interfere with mGluR5 internalization via interactions with  $\beta$ -arrestin, which is involved in mGluR5 re-cycling [19]. Higher levels of mGluR5 in selected neuronal populations might render them more sensitive to the effects of excitatory agonists, such as glutamate and potentially A $\beta$ .

The combined toxic effects of  $\alpha$ -syn and A $\beta$  via mGluR5 appeared to involve truncation of  $\alpha$ -syn mediated by calpain-I. Previous studies have shown that c-terminally truncated  $\alpha$ -syn is more prone to aggregate and to lead to neurotoxicity [52–55]. Both in the brains of patients with DLB/PD as well as in our  $\alpha$ -syn tg mice [51] and in BAC- $\alpha$ -syn rats [56], c-terminally truncated

$\alpha$ -syn is elevated. Among the proteases involved, calpain-I has been shown to play an important role [48]. The c-terminally truncated fragment we detected was consistent with calpain-I cleavage site as previously reported [51]. In our model, one possibility supported by the *in vitro* studies is that A $\beta$ / $\alpha$ -syn interacts with mGluR5 might result in increased intracellular calcium that in turn could activate calpain-I triggering  $\alpha$ -syn truncation and further aggregation. This is consistent with the known role of mGluR5 hyper-excitation mediated by A $\beta$  [42,57].

The role of mGluR5 in AD and PD has been the subject of considerable interest because of the potential for a therapeutic target [58]. It has been shown that in AD the A $\beta$  oligomers interact with mGluR5 [42,59] and that A $\beta$  dysregulates astroglial mGluR5 and calcium signaling [60]. In addition, inhibition of mGluR5 is neuroprotective against A $\beta$  toxicity [40] and mGluR5 is up regulated in Down syndrome [31]. In PD and related models, modulation of mGluR5 ameliorates the deficits in the MPTP treated mice [61] and 6-OH DOPA model [62].

Previous studies support the notion that  $\alpha$ -syn and A $\beta$  interact [63]. In Lewy body disease A $\beta$  deposition is associated with  $\alpha$ -syn lesions [9] and in crosses between PDGF-APP mutant and PDGF- $\alpha$ -syn, the  $\alpha$ -syn pathology and related deficits are exacerbated [12]. Similar results have been reported when crossing 3xTg-AD mice with mPrP- $\alpha$ -syn A53T tg mice [15] and between PDGF- $\alpha$ -syn and mThy1-APP mutant tg mice [13]. In addition,  $\alpha$ -syn mediated synapse damage is enhanced by A $\beta$  [64] and  $\alpha$ -syn and A $\beta$  cross-seed [13,14,65,66].

## Conclusions

In order to understand the role of  $\alpha$ -syn and A $\beta$  in mediating neurodegeneration in the hippocampus via mGluR5, we generated  $\alpha$ -syn/APP double tg mice by crossing mThy1- $\alpha$ -syn (Line 61) and mThy-1 APP (Line 41). In this model full-length  $\alpha$ -syn and mGluR5 were increased in the CA3 pyramidal layer of the hippocampus in  $\alpha$ -syn/APP mice compared to  $\alpha$ -syn tg mice. This was the same region of the hippocampus that was selectively vulnerable in APP,  $\alpha$ -syn, and  $\alpha$ -syn/APP tg mice. Lentivirus-mediated delivery of mGluR5 *in vivo* in the CA1 region, which was previously unaffected in the tg mice lines, led to increased vulnerability. Down-regulating or pharmacologically blocking mGluR5 protected hippocampal neurons from the neurotoxic effects of A $\beta$  and  $\alpha$ -syn. Further experiments suggested that the vulnerability of hippocampal neurons to  $\alpha$ -syn and A $\beta$  might be due to calcium influx mediated through mGluR5 via calpain and caspase-3 activation resulting in CT-truncation of  $\alpha$ -syn. Together, these results support the possibility that vulnerability of hippocampal neurons to  $\alpha$ -syn and A $\beta$  might be mediated via mGluR5. Moreover, therapeutical interventions targeting mGluR5 might have a role in DLB.

## Material and methods

### Generation of mThy-1 hAPP, ha-synuclein, and $\alpha$ -syn/APP transgenic mice

The University of California at San Diego's animal subjects committee approved all experiments. Mice expressing human (h) $\alpha$ -syn-bearing under the neuronal mThy-1 promoter cassette (provided by Dr. H. van der Putten, Ciba-Geigy, Basel, Switzerland) were generated as previously described [37]. Mice expressing hAPP751 cDNA containing the London (V717I) and Swedish-(K670M/N671L) mutations under the regulatory control of the murine (m)Thy-1 gene (mThy1-hAPP751) were generated as previously described [36]. These single tg mice were then cross-bred to generated mThy-1  $\alpha$ -syn/APP double tg mice.

### Construction of lentiviral vectors

The mouse mGluR5 cDNA was cloned into the 3<sup>rd</sup> generation lentivirus vector by PCR addition of the ApaI and BamHI restriction sites. This vector contains the human CMV promoter driving transgene expression and the WPRE element for increased mRNA stability. The sh-mGluR5 (GCA ACA TCC CGA ACA GT AA) was cloned into the pSI-H1-copGFP vector (SBI Vector) containing the H1 promoter. The control shRNA lentivector (LV-sh-Luc) contains an shRNA directed against firefly luciferase. Lentiviruses expressing - $\alpha$ -syn, mGluR5, sh-mGluR5, sh-luciferase or empty vector (as controls) was prepared by transient transfection in 293 T cells. The LV- $\alpha$ -syn has previously been characterized [67]. Lentivirus vectors were prepared by transient transfection of the 3 packaging plasmids and the vector plasmid in 293 T cells as previously described [68,69].

### Mouse lines and intracerebral injections of lentiviral vectors

A cohort of  $n = 48$  ( $n = 24$  LV-control and  $n = 24$  LV-mGluR5) mice were divided into the following groups: a) non-tg, b) APP, c)  $\alpha$ -syn and d)  $\alpha$ -syn/APP tg mice (6 month old,  $n = 6$  with LV-control and  $n = 6$  LV-mGluR5 per group), were injected with 3  $\mu$ L of the lentiviral preparations ( $2.5 \times 10^7$  TU) into the hippocampus CA1 region (using a 5  $\mu$ L Hamilton syringe). Similarly a cohort of  $n = 48$  were injected with LV-control ( $n = 24$ ) and LV-sh mGluR5 ( $n = 24$ ). Briefly, as previously described [70], mice were placed under anesthesia on a Kopf stereotaxic apparatus and coordinates (hippocampus: AP 2.0 mm, lateral 1.5 mm, depth 1.3 mm) were determined as per the Franklin and Paxinos atlas [71]. The lentiviral vectors were delivered using a Hamilton syringe connected to a hydraulic system to inject the solution at a rate of 1  $\mu$ L every 2 min. To allow diffusion of the solution into the brain tissue, the needle was left for

an additional 5 min after the completion of the injection. Mice survived for 3 months after the lentiviral injection.

### Tissue preparation

Following NIH guidelines for the humane treatment of animals, mice were anesthetized with chloral hydrate and flush-perfused transcardially with 0.9% saline. Brains were removed and divided in sagittal sections. The right hemi-brain was post-fixed in phosphate-buffered 4% PFA (pH7.4) at 4°C for 48 h for neuropathological analysis, while the left hemibrain was snap-frozen and stored at -70°C for subsequent RNA and protein analysis.

### RNA extraction and quantification of mRNA by real time-PCR analysis

RNA was extracted from mice in triplicate using the RNAeasy kit (QIAGEN, Germantown, MD, USA) [37], and quantified by spectrophotometer readings. For cDNA synthesis, 1 µg total RNA was reverse transcribed using iScript cDNA Synthesis kit (BioRad, Hercules, CA, USA). Real Time-PCR (RT-PCR) experiments were performed using the iQ5 Detection System (BioRad, Hercules, CA, USA). Amplification was performed on cDNA equivalent to 25 ng total RNA with 1 × iQ SYBRGreen Supermix (BioRad, Hercules, CA, USA). Template PCR reactions were performed in triplicate and run in duplicate using the following PCR cycling parameters: 50°C for 2 min, 95°C for 10 min, and 40 cycles of 94°C for 15 s, 60°C for 1 min followed by a dissociation protocol to verify the presence of a single product for each amplicon. The amount of cDNA was calculated by the comparative threshold cycle method and expressed using mouse actin as an internal control.

### Immunohistochemical analysis

Analysis was performed using free-floating, 40 µm thick, vibratome cut, blind-coded sections, as previously described [51,72]. Briefly, sections were incubated overnight at 4°C with antibodies against total α-syn (1:500, affinity purified rabbit polyclonal, Millipore) [73], C-terminus α-syn (SYN105, mouse monoclonal) [51], and mGluR5 (1:500; Millipore), followed by biotin-tagged anti-rabbit or anti-mouse IgG1 (1:100, Vector Laboratories, Inc., Burlingame, CA) secondary antibodies, Avidin D-HRP (1:200, ABC Elite, Vector), and visualized with diaminobenzidine (DAB). Background levels were obtained in tissue sections immunostained in the absence of primary antibody. Therefore: corrected optical density = optical density – background. Sections were scanned with a digital Olympus bright field digital microscope (BX41).

Analysis of neurodegenerative pathology was performed in vibratome sections immunolabeled with antibodies against the dendritic marker microtubule-associated protein-2 (MAP 2; 1:500, Millipore), pan-neuronal marker

NeuN (1:500, Millipore), astroglial marker glial fibrillary acidic protein (GFAP, 1:1000, Millipore) the microglial cell marker Iba-1 (Wako Laboratories, mouse monoclonal), activated caspase-3 (1:500; Cell Signaling) and synaptic marker synaptophysin (SY38, 1:500, Millipore) [51,73]. Sections reacted with antibodies against NeuN (1:4,000; Millipore), GFAP and Iba-1 were incubated with biotinylated secondary antibodies, Avidin D-HRP, and visualized with DAB. Sections reacted with antibodies against MAP 2 and synaptophysin were visualized with FITC-tagged secondary antibody or the Tyramide Signal Amplification™ Direct (Red) system (1:100, NEN Life Sciences, Boston, MA), respectively, mounted under glass coverslips with anti-fading media (Vector Laboratories), and imaged with the laser scanning confocal microscope (LSCM) (MRC1024, BioRad).

### Image analysis and stereology

Sections immunostained with antibodies against α-syn, mGluR5 and GFAP were analyzed with a digital Olympus bright field digital microscope (BX41). For each case a total of three sections (4 digital images per section at 400 × magnification) were obtained from the CA1 and CA3 region of the hippocampus and analyzed as previously described with the image J program (NIH) to obtain optical density, levels were corrected to background. Sections labeled with Iba-1, were analyzed utilizing the Image-Pro Plus program (Media Cybernetics, Silver Spring, MD) (10 digital images per section at 400 × magnification) and analyzed in order to estimate the average number of immuno-labeled cells per unit area (mm<sup>2</sup>) and the average intensity of the immunostaining (corrected optical density).

The numbers of NeuN-immunoreactive neurons were estimated utilizing unbiased stereological methods [74]. Hemisected brains were cut as serial sections and every 12th section containing the neocortex, hippocampus and striatum was outlined using an Olympus BX51 microscope running StereoInvestigator 8.21.1 software (MicroBrightField, Cochester, VT). Grid sizes for the hippocampal CA3 and CA1 pyramidal layers were: 150 × 150 and 300 × 300 µm, respectively and the counting frames were 30 × 30 and 50 × 50 µm, respectively. Perikarya within section approximately 480 µm apart were counted only if the first recognizable profile came into focus within the counting frame. A systematic sampling of the regions of interests was made from a random starting point. Full penetration of the section by the antibody was confirmed by focusing throughout the entire Z-axis. The average coefficient of error for each region was 0.09. Sections were analyzed using a 100 × 1.4 PlanApo oil-immersion objective. The average mounted tissue thickness was 10.1 µm, and a 5 µm high disector allowed for 2 µm top and bottom guard-zones.



Sections immunolabeled with antibodies against MAP 2 and synaptophysin were serially imaged with the LSCM (MRC1024, BioRad) and analyzed with the Image J program (NIH), as previously described [75]. For each mouse, a total of 3 sections were analyzed and for each section, 4 fields in the CA1 and CA3 of the hippocampus were examined. Results were expressed as percent area of the neuropil occupied.

#### Double immunolabeling and fluorescence co-labeling

To determine the co-localization between  $\alpha$ -syn and APP, as well as mGluR5 and cleaved caspase-3, double-labeling experiments were performed as previously [75]. Sections were immunolabeled with the following pairs of antibodies: a) human  $\alpha$ -syn (SYN211, mouse monoclonal, Millipore) and APP (6E10, mouse monoclonal Covance), b) human  $\alpha$ -syn (SYN211, mouse monoclonal, Millipore) and mGluR5 (Millipore, rabbit polyclonal) and c) cleaved caspase-3 (Cell Signaling, rabbit polyclonal) and C-terminal  $\alpha$ -syn (SYN105 mouse monoclonal). All sections were processed simultaneously, and experiments were performed in triplicate. The FL and CT  $\alpha$ -syn was detected with the Tyramide Red (NEN Life Sciences) whereas APP and mGluR5 were detected with FITC-tagged antibodies (1:75, Vector, Burlingame, CA). Sections were imaged with a Zeiss 63X1.4 objective on an Axiovert 35 microscope (Zeiss) with an attached MRC1024 laser scanning confocal microscope (LSCM) system (BioRad) [75].

#### Immunoblot analysis in co-immunoprecipitation

The levels of  $\alpha$ -syn, APP and mGluR5 in mouse brains, as well as the levels of  $\alpha$ -syn, mGluR5, brain spectrin and CT- $\alpha$ -syn in neuronal cultures were analyzed using lysate that were extracted and fractioned into soluble and insoluble fractions by ultracentrifugation [75]. Protein (20  $\mu$ g/lane) was loaded onto 4-12% SDS/PAGE gels and blotted onto PVDF membranes, incubated with specific antibodies, followed by HRP-tagged secondary antibodies (1:5,000; Santa Cruz Biotechnology). Bands were visualized by enhanced chemiluminescence (ECL, PerkinElmer, Boston, MA) and analyzed with a quantitative Versadoc XL imaging apparatus (BioRad).  $\beta$ -Actin (1:3,000) was the loading control.

To detect interactions between  $\alpha$ -syn and caspase-3 co-immunoprecipitation was performed as previously described [76] in neuronal cell lines infected with LV- $\alpha$ -syn and treated with A $\beta$  oligomers. Briefly, immunoprecipitation assays were carried out essentially as previously described [77]. The lysates were then centrifuged for 20 min at 12,000 rpm, and the protein concentrations were determined with a BCA protein assay kit. Three hundred  $\mu$ g of each of the supernatants was incubated with 1  $\mu$ g of the antibody against  $\alpha$ -syn, overnight at 4°C. Then the

immunocomplexes were adsorbed to protein A-Sepharose 4B or protein G-Sepharose (Amersham, Piscataway, NJ). After extensive washing with immunoprecipitation buffer, which contained 1% Trion X-100, samples were heated in NuPAGE SDS sample buffer (Invitrogen) for five min and subjected to gel electrophoresis on tris-tricine gels followed by immunoblot analysis with an antibody against caspase-3. The inverse immunoprecipitation with caspase-3 and immunoblotting with  $\alpha$ -syn was also performed.

#### Primary neuronal cultures treatments, lentiviral vectors and analysis

Hippocampal neuron cultures were prepared from P1 mouse hippocampi. Briefly, mouse hippocampi were dissected in HBSS dissecting media containing 4 mM NaHCO<sub>3</sub> (7.5%) and 10 mM HEPES buffer. Neurons were then dissociated by enzymatic treatment with 0.25% trypsin in dissecting media for 15 min at 37°C, and subsequent mechanical disruption. Neurons were plated at medium density (45,000 cells/cm<sup>2</sup>) on poly-L-lysine coated coverslips (12 mm in diameter) in MEM plating media containing 1 mM sodium pyruvate, 0.6% glucose, 10% horse serum, and 2 mM glutamine. Cultures were placed in an incubator at 37°C under a humidified atmosphere of 5% CO<sub>2</sub> in air for 2 hrs. The plating culture medium was then replaced and cultures were maintained in B27 supplemented Neurobasal media (Invitrogen) until 12 days *in vitro* (DIV). Primary neuronal cultures were infected with LV-control or LV- $\alpha$ -syn and with LV-sh-Luc or LV-mGluR5 after 48 hrs were treated with A $\beta$  oligomers as previously described [76]. Natural A $\beta$  was prepared according to Walsh et al. [78] (kindly provided by Dr. Eddie Koo) by incubating control CHO cells or CHO cells expressing APP V717F mutation (also referred as 7PA2 cells) with B27 conditioned media for 16 hrs. Total AB concentration was determined as previously described [79]. Neurons were treated with 80 pM of natural A $\beta$  for 24 hrs. Hippocampal neurons were plated on coverslips were rinsed briefly in PBS and fixed with 4% paraformaldehyde (PFA) and 4% sucrose in PBS-MC (phosphate buffered saline with 1 mM MgCl<sub>2</sub> and 0.1 CaCl<sub>2</sub>) for 10 min at room temperature. Neurons were then double immunolabeled as described above with antibodies against MAP 2 (Millipore) and  $\alpha$ -syn (SYN211, Millipore).  $\alpha$ -Syn was detected with the Tyramide Red (NEN Life Sciences) whereas MAP 2 was detected with FITC-tagged antibodies (1:75, Vector, Burlingame, CA). Coverslips were imaged with a Zeiss 63  $\times$  1.4 objective on an Axiovert 35 microscope (Zeiss) with an attached MRC1024 laser scanning confocal microscope (LSCM) system (BioRad) [75] and analyzed with Image J to determine neurite length and levels of  $\alpha$ -syn-ir (pixel intensity). The capacity of the LV-sh-mGluR5 at down-regulating mGluR5 was verified



in coverslips by immunocytochemistry with an antibody against mGluR5 detected with Tryamide Red and by immunoblot as described above.

#### Neuronal cell lines treatments, lentiviral vectors and analysis

The rat neuroblastoma cell line B103 was used for in vitro experiments because this cell line display neuronal features and we have shown that pathological features of synucleonopathies emerge when infected with LV- $\alpha$ -syn [69]. B103 cells were plated at  $3.5 \times 10^4$  cells/well on coverslips. After 6 hours cells were infected with LV-control, LV- $\alpha$ -syn (MOI = 50) and treated overnight later with A $\beta$  oligomers (1 nM). Cells were then fixed in 4% paraformaldehyde and analyzed by immunocytochemistry for the expression of  $\alpha$ -syn (Millipore), CT- $\alpha$ -syn (SYN105), caspase-3 (cell signaling) and mGluR5 (rabbit polyclonal) as described above. Cell lysates were divided by ultracentrifugation into soluble and insoluble fractions and analyzed by immunoblot for mGluR5, CT  $\alpha$ -syn,  $\alpha$ -syn and brain spectrin (Millipore) as described above.

To determine the involvement of mGluR5 in cytotoxicity, prior to the addition of A $\beta$  oligomers, sets of cells infected with LV-control and LV- $\alpha$ -syn were pre-treated for 6 hrs with the mGluR5 antagonists MPEP hydrochloride (50  $\mu$ M) (Tocris) and MTEP (50  $\mu$ M) (Millipore) or the mGluR5 agonist DHPG Dihydroxyphenylglycine (10  $\mu$ M) (Tocris) and analyzed for calcium levels and cytotoxicity. Cytotoxicity was assessed using the lactate dehydrogenase (LDH, CytoTox 96 assay, Promega) and MTT (3-(4,5-Dimethylthiazol-2-yl)-2,5-diphenyltetrazolium bromide, Roche) cell viability assays, as per manufacturer's instructions, to measure levels of cell death. Assessment of calcium influx was carried out as previously described [13] using a modified protocol of the FLIPR 4 calcium assay (Molecular Devices, Sunnyvale, CA). Briefly, B103 cells were infected with lentiviral constructs. Cells were infected at a MOI of 30, and two days after infection, cells were plated at a density of 30,000 cells/well on Costar 96 well-black plates with flat clear bottom (Corning). After an additional 24 hrs of incubation, media was replaced by 100  $\mu$ L of HBSS buffer, and 100  $\mu$ L of calcium dye (FLUO-4 NW, Invitrogen) was added to each well. Cells were kept in the incubator at 37°C for 30 mins, followed by incubation in the dark at room temperature for an additional 30 mins before measuring fluorescence with an excitation/emission filter at 470-495/515-575 nm on a DTX 880 Multimode Detector (Beckman Coulter). As a positive control of calcium influx, 0.6  $\mu$ g of ionomycin (Sigma, St. Louis, MO), was added to control wells.

Finally to ascertain the role of calpain-I and caspase-3 in neurotoxicity prior to the addition of A $\beta$  oligomers, were pre-treated for 6 hrs with the calpain-I inhibitor

calpastatin (50 nM) (Takeda) and the caspase-3 inhibitor N-Acetyl-Glu-Ser-Met-Asp-al (1  $\mu$ M) (Sigma) followed by analysis of cytotoxicity by LDH as described above.

#### Statistical analysis

All analyses used GraphPad Prism (version 5.0). Differences among means were assessed by one-way ANOVA with Dunnett's post-hoc test when compared to non-tg and by Tukey-Kramer when comparing tg groups. Two-way ANOVA with repeated measures followed by a Bonferroni multiple comparisons post-hoc test was used for analyzing the interactions between groups and time. The null hypothesis was rejected at the 0.05 level.

#### Competing interests

The authors declare that they have no competing interests.

#### Authors' contributions

CRO conceived and carried out the stereological studies and drafted the manuscript. AC performed in vitro studies with primary neuronal cell cultures. GS performed in vitro studies using neuroblastoma cell line. ER generated the tg mice and crosses. KU performed the initial characterization of the crosses. BS conceived/developed and performed experiments with mGluR5 and  $\alpha$ -syn lentiviruses. DP conceived the role of mGluR5 in DLB and contributed to in vitro characterization of mGluR5 levels. CP performed and analyzed the immunoassays and the in vivo analysis. PD designed and performed the in vitro calcium studies. EM conceived the idea, contributed to the writing, and performed confocal microscopy analysis. All authors read and approved the final manuscript.

#### Acknowledgements

This work was supported by NIH grants, AG18840, AG022074, and AG10435.

#### Author details

<sup>1</sup>Department of Neurosciences, University of California, San Diego, La Jolla, CA, USA. <sup>2</sup>Neuropore Therapies, Inc., San Diego, CA 92121, USA. <sup>3</sup>Department of Pathology, University of California, San Diego, La Jolla, CA, USA.

Received: 12 March 2014 Accepted: 13 May 2014

Published: 19 May 2014

#### References

1. As A: **Alzheimer's disease facts and figures.** *Alzheimer's Dementia* 2013, **2013**(9):1–71.
2. Masters CL, Selkoe DJ: **Biochemistry of amyloid beta-protein and amyloid deposits in Alzheimer disease.** *Cold Spring Harb Perspect Med* 2012, **2**:a006262.
3. Mucke L, Selkoe DJ: **Neurotoxicity of amyloid beta-protein: synaptic and network dysfunction.** *Cold Spring Harb Perspect Med* 2012, **2**:a006338.
4. Trojanowski J, Goedert M, Iwatsubo T, Lee V: **Fatal attractions: abnormal protein aggregation and neuron death in Parkinson's disease and lewy body dementia.** *Cell Death Differ* 1998, **5**:832–837.
5. Spillantini MG, Schmidt ML, Lee VM, Trojanowski JQ, Jakes R, Goedert M: **Alpha-synuclein in Lewy bodies.** *Nature* 1997, **388**:839–840.
6. Hashimoto M, Hernandez-Ruiz S, Hsu L, Sisk A, Xia Y, Takeda A, Sundsmo M, Masliah E: **Human recombinant NACP/a-synuclein is aggregated and fibrillated in vitro: relevance for Lewy body disease.** *Brain Res* 1998, **799**:301–306.
7. Lippa CF, Duda JE, Grossman M, Hurtig HI, Aarsland D, Boeve BF, Brooks DJ, Dickson DW, Dubois B, Emre M, Fahn S, Farmer JM, Galasko D, Galvin JE, Goetz CG, Growdon JH, Gwinn-Hardy KA, Hardy J, Heutink P, Iwatsubo T, Kosaka K, Lee VM, Leverenz JB, Masliah E, McKeith IG, Nussbaum RL, Olanow CW, Ravina BM, Singleton AB, Tanner CM, et al: **DLB and PDD boundary issues: diagnosis, treatment, molecular pathology, and biomarkers.** *Neurology* 2007, **68**:812–819.

8. McKeith IG: Consensus guidelines for the clinical and pathologic diagnosis of dementia with Lewy bodies (DLB): report of the Consortium on DLB International Workshop. *J Alzheimers Dis* 2006, **9**:417–423.
9. Pletnikova O, West N, Lee MK, Rudow GL, Skolasky RL, Dawson TM, Marsh L, Troncoso JC: Abeta deposition is associated with enhanced cortical alpha-synuclein lesions in Lewy body diseases. *Neurobiol Aging* 2005, **26**:1183–1192.
10. Lippa CF, Fujiwara H, Mann DM, Giasson B, Baba M, Schmidt ML, Nee LE, O'Connell B, Pollen DA, St George-Hyslop P, Ghetti B, Nochlin D, Bird TD, Cairns NJ, Lee VM, Iwatsubo T, Trojanowski JQ: Lewy bodies contain altered alpha-synuclein in brains of many familial Alzheimer's disease patients with mutations in presenilin and amyloid precursor protein genes. *Am J Pathol* 1998, **153**:1365–1370.
11. Morales R, Moreno-Gonzalez I, Soto C: Cross-seeding of misfolded proteins: implications for etiology and pathogenesis of protein misfolding diseases. *PLoS Pathog* 2013, **9**:e1003537.
12. Masliah E, Rockenstein E, Veinbergs I, Sagara Y, Mallory M, Hashimoto M, Mucke L: beta-amyloid peptides enhance alpha-synuclein accumulation and neuronal deficits in a transgenic mouse model linking Alzheimer's disease and Parkinson's disease. *Proc Natl Acad Sci U S A* 2001, **98**:12245–12250.
13. Tsigenly IF, Crews L, Desplats P, Shaked GM, Sharikov Y, Mizuno H, Spencer B, Rockenstein E, Trejo M, Platoshy O, Yuan JX, Masliah E: Mechanisms of hybrid oligomer formation in the pathogenesis of combined Alzheimer's and Parkinson's diseases. *PLoS One* 2008, **3**:e3135.
14. Mandal PK, Pettegrew JW, Masliah E, Hamilton RL, Mandal R: Interaction between Abeta peptide and alpha synuclein: molecular mechanisms in overlapping pathology of Alzheimer's and Parkinson's in dementia with Lewy body disease. *Neurochem Res* 2006, **31**:1153–1162.
15. Clinton LK, Blurton-Jones M, Myszcz K, Trojanowski JQ, LaFerla FM: Synergistic interactions between Abeta, tau, and alpha-synuclein: acceleration of neuropathology and cognitive decline. *J Neurosci* 2010, **30**:7281–7289.
16. Hamilton RL: Lewy bodies in Alzheimer's disease: a neuropathological review of 145 cases using alpha-synuclein immunohistochemistry. *Brain Pathol* 2000, **10**:378–384.
17. Zaja-Milatovic S, Keene CD, Montine KS, Leverenz JB, Tsuang D, Montine TJ: Selective dendritic degeneration of medium spiny neurons in dementia with Lewy bodies. *Neurology* 2006, **66**:1591–1593.
18. Harding AJ, Lakay B, Halliday GM: Selective hippocampal neuron loss in dementia with Lewy bodies. *Ann Neurol* 2002, **51**:125–128.
19. Price DL, Rockenstein E, Ubhi K, Phung V, MacLean-Lewis N, Askay D, Cartier A, Spencer B, Patrick C, Desplats P, Ellisman MH, Masliah E: Alterations in mGluR5 expression and signaling in Lewy body disease and in transgenic models of alpha-synucleinopathy—implications for excitotoxicity. *PLoS One* 2010, **5**:e14020.
20. Caraci F, Battaglia G, Sortino MA, Spampinato S, Molinaro G, Copani A, Nicoletti F, Bruno V: Metabotropic glutamate receptors in neurodegeneration/neuroprotection: still a hot topic? *Neurochem Int* 2012, **61**:559–565.
21. Lee HG, Zhu X, O'Neill MJ, Webber K, Casadesus G, Marlatt M, Raina AK, Perry G, Smith MA: The role of metabotropic glutamate receptors in Alzheimer's disease. *Acta Neurobiol Exp (Wars)* 2004, **64**:89–98.
22. Marino MJ, Valenti O, Conn PJ: Glutamate receptors and Parkinson's disease: opportunities for intervention. *Drugs Aging* 2003, **20**:377–397.
23. Feeley Kearney JA, Albin RL: mGluRs: a target for pharmacotherapy in Parkinson disease. *Exp Neurol* 2003, **184**(Suppl 1):S30–S36.
24. Naie K, Manahan-Vaughan D: Regulation by metabotropic glutamate receptor 5 of LTP in the dentate gyrus of freely moving rats: relevance for learning and memory formation. *Cereb Cortex* 2004, **14**:189–198.
25. Simonyi A, Schachman TR, Christoffersen GR: The role of metabotropic glutamate receptor 5 in learning and memory processes. *Drug News Perspect* 2005, **18**:353–361.
26. Romano C, Sesma MA, McDonald CT, O'Malley K, Van den Pol AN, Olney JW: Distribution of metabotropic glutamate receptor mGluR5 immunoreactivity in rat brain. *J Comp Neurol* 1995, **355**:455–469.
27. Marino MJ, Awad H, Poisk O, Wittmann M, Conn PJ: Localization and physiological roles of metabotropic glutamate receptors in the direct and indirect pathways of the basal ganglia. *Amino Acids* 2002, **23**:185–191.
28. Conn PJ, Battaglia G, Marino MJ, Nicoletti F: Metabotropic glutamate receptors in the basal ganglia motor circuit. *Nat Rev Neurosci* 2005, **6**:787–798.
29. Albasanz JL, Dalfó E, Ferrer I, Martin M: Impaired metabotropic glutamate receptor/phospholipase C signaling pathway in the cerebral cortex in Alzheimer's disease and dementia with Lewy bodies correlates with stage of Alzheimer's-disease-related changes. *Neurobiol Dis* 2005, **20**:685–693.
30. Tyszkiewicz JP, Yan Z: beta-Amyloid peptides impair PKC-dependent functions of metabotropic glutamate receptors in prefrontal cortical neurons. *J Neurophysiol* 2005, **93**:3102–3111.
31. Oka A, Takashima S: The up-regulation of metabotropic glutamate receptor 5 (mGluR5) in Down's syndrome brains. *Acta Neuropathol (Berl)* 1999, **97**:275–278.
32. Battaglia G, Busceti CL, Molinaro G, Biagioni F, Storto M, Fornai F, Nicoletti F, Bruno V: Endogenous activation of mGlu5 metabotropic glutamate receptors contributes to the development of nigro-striatal damage induced by 1-methyl-4-phenyl-1,2,3,6-tetrahydropyridine in mice. *J Neurosci* 2004, **24**:828–835.
33. Flor PJ, Battaglia G, Nicoletti F, Gasparini F, Bruno V: Neuroprotective activity of metabotropic glutamate receptor ligands. *Adv Exp Med Biol* 2002, **513**:197–223.
34. Aguirre JA, Kehr J, Yoshitake T, Liu FL, Rivera A, Fernandez-Espinola S, Andbjør B, Leo G, Medhurst AD, Agnati LF, Fuxe K: Protection but maintained dysfunction of nigral dopaminergic nerve cell bodies and striatal dopaminergic terminals in MPTP-lesioned mice after acute treatment with the mGluR5 antagonist MPEP. *Brain Res* 2005, **1033**:216–220.
35. Vernon AC, Palmer S, Datla KP, Zbarsky V, Croucher MJ, Dexter DT: Neuroprotective effects of metabotropic glutamate receptor ligands in a 6-hydroxydopamine rodent model of Parkinson's disease. *Eur J Neurosci* 2005, **22**:1799–1806.
36. Rockenstein E, Mallory M, Mante M, Sisk A, Masliah E: Early formation of mature amyloid-beta protein deposits in a mutant APP transgenic model depends on levels of Abeta(1–42). *J Neurosci Res* 2001, **66**:573–582.
37. Rockenstein E, Mallory M, Hashimoto M, Song D, Shults CW, Lang I, Masliah E: Differential neuropathological alterations in transgenic mice expressing alpha-synuclein from the platelet-derived growth factor and Thy-1 promoters. *J Neurosci Res* 2002, **68**:568–578.
38. Movsesyan VA, Stoica BA, Faden AI: MGLuR5 activation reduces beta-amyloid-induced cell death in primary neuronal cultures and attenuates translocation of cytochrome c and apoptosis-inducing factor. *J Neurochem* 2004, **89**:1528–1536.
39. Wang Q, Walsh DM, Rowan MJ, Selkoe DJ, Anwyl R: Block of long-term potentiation by naturally secreted and synthetic amyloid beta-peptide in hippocampal slices is mediated via activation of the kinases c-Jun N-terminal kinase, cyclin-dependent kinase 5, and p38 mitogen-activated protein kinase as well as metabotropic glutamate receptor type 5. *J Neurosci* 2004, **24**:3370–3378.
40. Liu F, Gong X, Zhang G, Marquis K, Reinhart P, Andree TH: The inhibition of glycogen synthase kinase 3beta by a metabotropic glutamate receptor 5 mediated pathway confers neuroprotection to Abeta peptides. *J Neurochem* 2005, **95**:1363–1372.
41. Blanchard BJ, Thomas VL, Ingram VM: Mechanism of membrane depolarization caused by the Alzheimer Abeta1–42 peptide. *Biochem Biophys Res Commun* 2002, **293**:1197–1203.
42. Renner M, Lacor PN, Velasco PT, Xu J, Contractor A, Klein WL, Triller A: Deleterious effects of amyloid beta oligomers acting as an extracellular scaffold for mGluR5. *Neuron* 2010, **66**:739–754.
43. Lea PM, Movsesyan VA, Faden AI: Neuroprotective activity of the mGluR5 antagonists MPEP and MTEP against acute excitotoxicity differs and does not reflect actions at mGluR5 receptors. *Br J Pharmacol* 2005, **145**:527–534.
44. Danzer KM, Haasen D, Karow AR, Moussaud S, Habeck M, Giese A, Kretschmar H, Hengerer B, Kostka M: Different species of alpha-synuclein oligomers induce calcium influx and seeding. *J Neurosci* 2007, **27**:9220–9232.
45. Arispe N, Rojas E, Pollard HB: Alzheimer disease amyloid beta protein forms calcium channels in bilayer membranes: blockade by tromethamine and aluminum. *Proc Natl Acad Sci U S A* 1993, **90**:567–571.
46. Kawahara M, Negishi-Kato M, Sadakane Y: Calcium dyshomeostasis and neurotoxicity of Alzheimer's beta-amyloid protein. *Expert Rev Neurother* 2009, **9**:681–693.
47. Dufty BM, Warner LR, Hou ST, Jiang SX, Gomez-Isla T, Leenhouts KM, Oxford JT, Feany MB, Masliah E, Rohn TT: Calpain-cleavage of [alpha]-synuclein: connecting proteolytic processing to disease-linked aggregation. *Am J Pathol* 2007, **170**:1725–1738.

48. Mishizen-Eberz AJ, Guttman RP, Giasson BI, Day GA 3rd, Hodara R, Ischiropoulos H, Lee VM, Trojanowski JQ, Lynch DR: **Distinct cleavage patterns of normal and pathologic forms of alpha-synuclein by calpain in vitro.** *J Neurochem* 2003, **86**:836–847.
49. Mishizen-Eberz AJ, Norris EH, Giasson BI, Hodara R, Ischiropoulos H, Lee VM, Trojanowski JQ, Lynch DR: **Cleavage of alpha-synuclein by calpain: potential role in degradation of fibrillized and nitrated species of alpha-synuclein.** *Biochemistry* 2005, **44**:7818–7829.
50. Kim SJ, Sung JY, Um JW, Hattori N, Mizuno Y, Tanaka K, Paik SR, Kim J, Chung KC: **Parkin cleaves intracellular alpha-synuclein inclusions via the activation of calpain.** *J Biol Chem* 2003, **278**:41890–41899.
51. Games D, Seubert P, Rockenstein E, Patrick C, Trejo M, Ubhi K, Etle B, Ghassemian M, Barbour R, Schenk D, Nuber S, Masliah E: **Axonopathy in an alpha-synuclein transgenic model of Lewy body disease is associated with extensive accumulation of C-terminal-truncated alpha-synuclein.** *Am J Pathol* 2013, **182**:940–953.
52. Luk KC, Kehm VM, Zhang B, O'Brien P, Trojanowski JQ, Lee VM: **Intracerebral inoculation of pathological alpha-synuclein initiates a rapidly progressive neurodegenerative alpha-synucleinopathy in mice.** *J Exp Med* 2012, **209**:975–986.
53. Tofaris GK, Garcia Reitbock P, Humby T, Lambourne SL, O'Connell M, Ghetti B, Gossage H, Emson PC, Wilkinson LS, Goedert M, Spillantini MG: **Pathological changes in dopaminergic nerve cells of the substantia nigra and olfactory bulb in mice transgenic for truncated human alpha-synuclein(1–120): implications for Lewy body disorders.** *J Neurosci* 2006, **26**:3942–3950.
54. Ulusoy A, Febbraro F, Jensen PH, Kirik D, Romero-Ramos M: **Co-expression of C-terminal truncated alpha-synuclein enhances full-length alpha-synuclein-induced pathology.** *Eur J Neurosci* 2010, **32**:409–422.
55. Daher JP, Ying M, Banerjee R, McDonald RS, Hahn MD, Yang L, Flint Beal M, Thomas B, Dawson VL, Dawson TM, Moore DJ: **Conditional transgenic mice expressing C-terminally truncated human alpha-synuclein (alpha-Syn119) exhibit reduced striatal dopamine without loss of nigrostriatal pathway dopaminergic neurons.** *Mol Neurodegener* 2009, **4**:34.
56. Nuber S, Harmuth F, Kohl Z, Adame A, Trejo M, Schonig K, Zimmermann F, Bauer C, Casadei N, Giel C, Calaminus C, Pichler BJ, Jensen PH, Muller CP, Amato D, Kornhuber J, Teismann P, Yamakado H, Takahashi R, Winkler J, Masliah E, Riess O: **A progressive dopaminergic phenotype associated with neurotoxic conversion of alpha-synuclein in BAC-transgenic rats.** *Brain* 2013, **136**:412–432.
57. Grolla AA, Sim JA, Lim D, Rodriguez JJ, Genazzani AA, Verkhratsky A: **Amyloid-beta and Alzheimer's disease type pathology differentially affects the calcium signalling toolkit in astrocytes from different brain regions.** *Cell Death Dis* 2013, **4**:e623.
58. Cleva RM, Olive MF: **Positive allosteric modulators of type 5 metabotropic glutamate receptors (mGluR5) and their therapeutic potential for the treatment of CNS disorders.** *Molecules* 2011, **16**:2097–2106.
59. Um JW, Kaufman AC, Kostylev M, Heiss JK, Stagi M, Takahashi H, Kerrisk ME, Vortmeyer A, Wisniewski T, Koleske AJ, Gunther EC, Nygaard HB, Strittmatter SM: **Metabotropic glutamate receptor 5 is a coreceptor for Alzheimer abeta oligomer bound to cellular prion protein.** *Neuron* 2013, **79**:887–902.
60. Lim D, Iyer A, Ronco V, Grolla AA, Canonico PL, Aronica E, Genazzani AA: **Amyloid beta deregulates astroglial mGluR5-mediated calcium signaling via calcineurin and NF-kB.** *Glia* 2013, **61**:1134–1145.
61. Hsieh MH, Ho SC, Yeh KY, Pawlak CR, Chang HM, Ho YJ, Lai TJ, Wu FY: **Blockade of metabotropic glutamate receptors inhibits cognition and neurodegeneration in an MPTP-induced Parkinson's disease rat model.** *Pharmacol Biochem Behav* 2012, **102**:64–71.
62. Black YD, Xiao D, Pellegrino D, Kachroo A, Brownell AL, Schwarzschild MA: **Protective effect of metabotropic glutamate mGluR5 receptor elimination in a 6-hydroxydopamine model of Parkinson's disease.** *Neurosci Lett* 2010, **486**:161–165.
63. Marsh SE, Blurton-Jones M: **Examining the mechanisms that link beta-amyloid and alpha-synuclein pathologies.** *Alzheimers Res Ther* 2012, **4**:11.
64. Bate C, Gentleman S, Williams A: **alpha-synuclein induced synapse damage is enhanced by amyloid-beta1-42.** *Mol Neurodegener* 2010, **5**:55.
65. Ono K, Takahashi R, Ikeda T, Yamada M: **Cross-seeding effects of amyloid beta-protein and alpha-synuclein.** *J Neurochem* 2012, **122**:883–890.
66. Henning Jensen P: **alpha-Synuclein/Amyloid Interactions.** *Methods Mol Med* 2001, **62**:61–65.
67. Bar-On P, Crews L, Koob AO, Mizuno H, Adame A, Spencer B, Masliah E: **Statins reduce neuronal alpha-synuclein aggregation in vitro models of Parkinson's disease.** *J Neurochem* 2008, **105**:1656–1667.
68. Tiscornia G, Singer O, Verma IM: **Design and cloning of lentiviral vectors expressing small interfering RNAs.** *Nat Protoc* 2006, **1**:234–240.
69. Spencer B, Potkar R, Trejo M, Rockenstein E, Patrick C, Gindi R, Adame A, Wyss-Coray T, Masliah E: **Bedlin 1 gene transfer activates autophagy and ameliorates the neurodegenerative pathology in alpha-synuclein models of Parkinson's and Lewy body diseases.** *J Neurosci* 2009, **29**:13578–13588.
70. Marr RA, Rockenstein E, Mukherjee A, Kindy MS, Hersh LB, Gage FH, Verma IM, Masliah E: **Nephrilysin gene transfer reduces human amyloid pathology in transgenic mice.** *J Neurosci* 2003, **23**:1992–1996.
71. Franklin KBJ, Paxinos G: *The mouse brain in stereotaxic coordinates.* San Diego: Academic Press; 1997.
72. Zwilling D, Huang SY, Sathyaikumar KV, Notarangelo FM, Guidetti P, Wu HQ, Lee J, Truong J, Andrews-Zwilling Y, Hsieh EW, Louie JY, Wu T, Searce-Lewie K, Patrick C, Adame A, Giorgini F, Moussaoui S, Laue G, Rassoulpour A, Flik G, Huang Y, Muchowski JM, Masliah E, Schwarcz R, Muchowski PJ: **Kynurenine 3-monooxygenase inhibition in blood ameliorates neurodegeneration.** *Cell* 2011, **145**:863–874.
73. Masliah E, Rockenstein E, Veinbergs I, Mallory M, Hashimoto M, Takeda A, Sagara Y, Sisk A, Mucke L: **Dopaminergic loss and inclusion body formation in alpha-synuclein mice: implications for neurodegenerative disorders.** *Science* 2000, **287**:1265–1269.
74. Overk CR, Kelley CM, Mufson EJ: **Brainstem Alzheimer's-like pathology in the triple transgenic mouse model of Alzheimer's disease.** *Neurobiol Dis* 2009, **35**:415–425.
75. Masliah E, Rockenstein E, Mante M, Crews L, Spencer B, Adame A, Patrick C, Trejo M, Ubhi K, Rohn TT, Mueller-Streicher S, Seubert P, Barbour R, McConlogue L, Buttini M, Games D, Schenk D: **Passive immunization reduces behavioral and neuropathological deficits in an alpha-synuclein transgenic model of Lewy body disease.** *PLoS One* 2011, **6**:e19338.
76. Pham E, Crews L, Ubhi K, Hansen L, Adame A, Cartier A, Salmon D, Galasko D, Michael S, Savas JN, Yates JR, Glabe C, Masliah E: **Progressive accumulation of amyloid-beta oligomers in Alzheimer's disease and in amyloid precursor protein transgenic mice is accompanied by selective alterations in synaptic scaffold proteins.** *FEBS J* 2010, **277**:3051–3067.
77. Hashimoto M, Rockenstein E, Mante M, Mallory M, Masliah E: **b-Synuclein inhibits alpha-synuclein aggregation: a possible role as an anti-parkinsonian factor.** *Neuron* 2001, **32**:213–223.
78. Walsh DM, Klyubin I, Fadeeva JV, Cullen WK, Anwyl R, Wolfe MS, Rowan MJ, Selkoe DJ: **Naturally secreted oligomers of amyloid beta protein potently inhibit hippocampal long-term potentiation in vivo.** *Nature* 2002, **416**:535–539.
79. Levites Y, Das P, Price RW, Rochette MJ, Kostura LA, McGowan EM, Murphy MP, Golde TE: **Anti-Abeta42- and anti-Abeta40-specific mAbs attenuate amyloid deposition in an Alzheimer disease mouse model.** *J Clin Invest* 2006, **116**:193–201.

doi:10.1186/1750-1326-9-18

**Cite this article as:** Overk et al.: Hippocampal neuronal cells that accumulate alpha-synuclein fragments are more vulnerable to Aβ oligomer toxicity via mGluR5 – implications for dementia with Lewy bodies. *Molecular Neurodegeneration* 2014 **9**:18.

**Submit your next manuscript to BioMed Central and take full advantage of:**

- **Convenient online submission**
- **Thorough peer review**
- **No space constraints or color figure charges**
- **Immediate publication on acceptance**
- **Inclusion in PubMed, CAS, Scopus and Google Scholar**
- **Research which is freely available for redistribution**

Submit your manuscript at  
www.biomedcentral.com/submit

